Ghrelin's orexigenic action in the lateral hypothalamic area involves indirect recruitment of orexin neurons and arcuate nucleus activation

Franco Barrile, Daniela Cassano, Gimena Fernandez, Pablo N de Francesco, Mirta Reynaldo, Sonia Cantel, Jean-Alain Fehrentz, José Donato, Helgi B Schiöth, Jeffrey M Zigman, et al.

GHRELIN'S OREXIGENIC ACTION IN THE LATERAL HYPOTHALAMIC AREA INVOLVES INDIRECT RECRUITMENT OF OREXIN NEURONS AND ARCUATE NUCLEUS ACTIVATION

Franco Barrile[1], Daniela Cassano[1], Gimena Fernandez[1], Pablo N. De Francesco[1], Mirta Reynaldo[1], Sonia Cantel[2],Jean-Alain Fehrentz[2], José Donato Jr[3], Helgi B. Schiöth[5], Jeffrey M. Zigman[4], Mario Perello[1,5]

[1] Laboratory of Neurophysiology of the Multidisciplinary Institute of Cell Biology [IMBICE, Argentine Research Council (CONICET) and Scientific Research Commission, Province of Buenos Aires (CIC-PBA), National University of La Plata], La Plata, Buenos Aires, Argentina.

[2] IBMM, UMR 5247, Univ Montpellier, CNRS, ENSCM, Montpellier, France.

[3] Department of Physiology and Biophysics, Instituto de Ciencias Biomedicas, Universidade de São Paulo, São Paulo, Brazil.

[4] Center for Hypothalamic Research, Department of Internal Medicine, UT Southwestern Medical Center, Dallas, Texas, USA.

[5] Department of Surgical Sciences, Functional Pharmacology and Neuroscience, University of Uppsala, Uppsala, Sweden.

Short title: GHSR neurons in the mouse LHA

Corresponding Author:
Dr. Mario Perelló
Laboratory of Neurophysiology, Multidisciplinary Institute of Cell Biology
Calle 526 S/N entre 10 y 11. La Plata, Buenos Aires, Argentina 1900
Phone +54 221 4210112
Email: mperello@imbice.gov.ar

The authors have nothing to disclose.
Keywords: GHSR, food intake, LHA, AgRP neurons.
Number of Figures: 8

ABSTRACT

Objective: Ghrelin is a potently orexigenic hormone, and a putative target mediating ghrelin's effects on food intake is the lateral hypothalamic area (LHA). Since the neurobiological basis of ghrelin's actions in the hypothalamic area have been poorly studied, we aimed to investigate the presence of neurons expressing ghrelin receptor (a.k.a. growth hormone secretagogue receptor, GHSR) in the mouse LHA (LHA^{GHSR} neurons), its physiological implications and the neuronal circuit recruited by local ghrelin action.

Methods: We investigated the distribution of LHA^{GHSR} neurons using different histologic strategies, including reporter mice expressing enhanced green fluorescent protein under the control of the GHSR promoter. Also, we investigated the physiological implications of local action of ghrelin within the LHA, and the extent to which the orexigenic effect of intra-LHA injected ghrelin involves the arcuate nucleus (ARH) and orexin neurons of the LHA (LHA^{orexin} neurons)

Results: We found that: 1) LHA^{GHSR} neurons are homogeneously distributed throughout the entire LHA; 2) intra-LHA injections of ghrelin transiently increase food intake and locomotor activity; 3) ghrelin's orexigenic effect in the LHA involves the indirect recruitment of LHA^{orexin} neurons and the activation of ARH neurons; and 4) LHA^{GHSR} neurons are not targeted by plasma ghrelin.

Conclusions: We provide a compelling neuroanatomical and functional characterization of LHA^{GHSR} neurons in male mice that indicates that LHA^{GHSR} cells are part of a hypothalamic neuronal circuit that potently induces food intake.

INTRODUCTION

The stomach-derived acylated peptide ghrelin is recognized as the most potently known orexigenic hormone [1]. A ghrelin bolus in satiated humans has consistently been shown to increase appetite sensations and food intake [2]. Also, a single systemic injection of ghrelin induces a rapid and robust increase of food intake in *ad libitum* fed mice and other rodent species [3]. Such a potent orexigenic effect has made ghrelin an attractive candidate for therapeutics aimed to treat conditions in which increasing caloric intake is important, such as anorexia nervosa or cancer-induced cachexia [4]. However, taking advantage of ghrelin's orexigenic effects has been challenging as ghrelin also affects a plethora of other physiological processes including the neuroendocrine axis, glucose homeostasis, and complex cognitive functions, such as reward-related behaviors [1, 5, 6]. Thus, understanding the precise neurobiological basis mediating ghrelin's orexigenic effects is crucial for the development of selective ghrelin mimetics displaying minimal unwanted effects.

The neuronal circuits and the molecular mechanisms mediating ghrelin's orexigenic effects have been extensively studied in the past decades [3, 7–9]. Ghrelin acts via the growth hormone secretagogue receptor (GHSR), which is highly expressed in most brain areas known to regulate food intake [10]. For instance, it is well established that ghrelin-induced food intake involves hypothalamic arcuate nucleus (ARH) neurons producing the orexigenic neuropeptides neuropeptide Y (NPY) and agouti-related protein (AgRP), hereafter named $ARH^{NPY/AgRP}$ neurons, which highly express GHSR and sense plasma ghrelin levels [3, 7, 8, 11]. Also, ghrelin regulates food intake by recruiting neuronal sets of the mesolimbic pathway, including the dopamine neurons of the ventral tegmental area (VTA) [12, 13], and affecting food reward-related behaviors [5, 14]. On top of these more systematically investigated targets mediating ghrelin's orexigenic effects, ghrelin has been shown to be able to locally act in some specific brain regions of rodents to induce feeding [15, 16]. In this regard, some studies showed that local injection of ghrelin in the lateral hypothalamic area (LHA) induces feeding [17, 18]. A putative role for the LHA mediating ghrelin's orexigenic effects is not surprising as this hypothalamic area has been classically recognized as a "feeding center" based on the seminal studies published in the 50s showing that bilateral LHA lesion in rats induces aphagia [19, 20]. However, the neuronal circuit mediating the orexigenic effect of ghrelin in the LHA and its implications as a target of ghrelin have been investigated in very few studies.

The LHA is a large hypothalamic region comprised of multiple and partially segregated cell types that, in turn, are interconnected with numerous intra- and extra-hypothalamic centers [21–23]. GHSR mRNA was found in the LHA of rats using either *in situ* hybridization histochemistry (ISHH) [24, 25] or qPCR [17]. The study of the presence of GHSR in the mouse LHA, however, have resulted in controversial observations. Our initial analysis of the distribution of GHSR mRNA throughout the entire mouse brain using ISHH did not reveal labeling in the LHA [26]. Conversely, we did observe fluorescent neurons in the LHA of reporter mice generated by crossing a GHSR-Cre mouse line, which express Cre recombinase under the control of GHSR promoter, with different reporter mice [27]. It seems evident that confirming the presence of the GHSR-expressing neurons in the mouse LHA, hereafter named LHA^{GHSR} neurons, is important as mouse models have been instrumental to decipher the neuronal circuits that control food intake in mammals. In order to precisely establish the presence and neuroanatomical distribution of the LHA^{GHSR} neurons in mice, the current study takes advantage of a reporter mouse line that expresses enhanced green fluorescent protein (eGFP) in GHSR-expressing cells ($GHSR^{eGFP}$ mice), which have been validated by us in the past, but not used to explicitly analyze the LHA [28].

In rats, intra-LHA infusion of ghrelin increases food intake [18, 29], and centrally-injected ghrelin increases the expression of the marker of cellular activation c-Fos in the LHA [18, 30, 31]. In mice, centrally-injected ghrelin also induces c-Fos in the LHA [32]. To our knowledge, however, the ability of ghrelin to directly act in the mouse LHA and its functional implications have not been reported. Importantly, studies in mice have systematically shown that some of ghrelin's actions involve the orexin neurons of the LHA, hereafter named LHA^{orexin} neurons and a.k.a. hypocretin neurons. For instance, centrally-injected ghrelin induces c-Fos in LHA^{orexin} neurons [30, 33] and the orexigenic effect of centrally-injected ghrelin is reduced in wild-type mice treated with anti-orexin antibodies and in orexin-knock out mice [30]. In addition, ghrelin actions enhancing either the motivation for high-fat diet or it´s rewarding value are impaired in mice with pharmacological or genetic blockage of the LHA^{orexin} signaling [34]. Thus, the current study was aimed to investigate the role of the LHA as a target of ghrelin in mice and to specifically assess the extent to which LHA^{orexin} neurons are involved in such actions.

MATERIALS AND METHODS

1. Animals. Adult male (8-10-week-old) *Mus musculus* mice produced at the IMBICE or UT Southwestern Medical Center animal facilities were used for the study. Housing temperature (21±1°C) and photoperiod (12-hour light/dark cycle from 7:00 to 19:00 h) were controlled and regular chow and water were available *ad libitum*, except when indicated. Experimental mice included: 1) Wild-type (WT) C57BL/6 mice; 2) $GHSR^{eGFP}$ mice (Mutant Mouse Resource & Research Center, Tg(Ghsr)-EGFP KZ65Gsat; Stock 030942), which express eGFP under the control of GHSR promoter [28], 3) NPY-humanized *Renilla reniformis* GFP (NPY^{hrGFP}) mice (Jackson Laboratory, Stock 006417), which express the hrGFP under the control of NPY promoter [35] and 4) $GHSR^{eGFP/}Gad2^{tdTomato}$ mice, which express eGFP in GHSR-expressing cells and tdTomato fluorescent protein in glutamate decarboxylase 2 (Gad2)-expressing gamma-aminobutyric acid (GABA) cells. $GHSR^{eGFP/}Gad2^{tdTomato}$ mice were generated by crossing $Gad2^{tdTomato}$ mice and $GHSR^{eGFP}$ mice. $Gad2^{tdTomato}$ mice were, in turn, generated from crosses between the Ai14 reporter mice (Allen Institute, 129S6-Gt(ROSA)26Sor$^{tm14(CAGtdTomato)Hze}$/J; Stock 007908) mice [36, 37] and Gad2-CreER mice (Jackson Laboratory, Gad2$^{tm1(cre/ERT2)Zjh}$/J; Stock 010702), which express a tamoxifen-inducible Cre recombinase under the control of Gad2 promoter [38]. Adult $GHSR^{eGFP}/Gad2^{tdTomato}$ mice received daily injections of tamoxifen (Sigma-Aldrich, cat. T5648; 70 mg/kg body weight (BW), intraperitoneal (IP)) for 3 consecutive days to induce the Cre recombination, and used 3 weeks later. All genetically modified mice were backcrossed for more than 10 generations onto a C57BL/6 genetic background. In order to generate ARH-ablated mice, 4-day-old WT pups were subcutaneously injected with monosodium glutamate (2 mg/g BW, Sigma-Aldrich, Cat. G1626) or saline (ARH-intact mice). The ablation of the ARH was histologically confirmed, as previously described [32] All protocols received approval from the Institutional Animal Care and Use Committee of the IMBICE and UT Southwestern Medical Center.

2. Perfusion and processing of brain samples. Mice were anesthetized and perfused using formalin, as previously described [39]. Then, brains were removed, post-fixed in formalin for 2 h at 4°C and immersed in 20% sucrose in phosphate-buffered saline (PBS, pH 7.4), at 4°C overnight. Next day, brains were frozen and serially cut on a cryostat into

four interleaving equivalent series of 40 µm coronal sections. Brain sections were stored in cryopreservant solution at −20°C until further histological processing.

3. In situ hybridization histochemistry (ISHH) for GHSR. Brain sections were subjected ISHH using procedures reported previously [28]. Briefly, sections were pretreated with 0.1% sodium borohydride for 15 minutes at room temperature. After washing, sections were rinsed in 0.1 M triethanolamine (TEA, pH 8.0), incubated in 0.25% acetic anhydride in 0.1 M TEA for 10 min, then washed again in 2X saline-sodium citrate buffer (SSC). Sections were then incubated at 50°C for 16 h with 33P-labeled mouse GHSR riboprobe diluted to 10^6 cpm/mL in hybridization solution [40]. Subsequently, sections were rinsed in 4X SSC and incubated in 0.002% RNase A solution for 30 min at 37°C. Sections were then rinsed in 2X SSC and submitted to sequential stringency washes with 2X SSC and 0.2X SSC for 1 h each at 55°C. Next, sections were mounted onto SuperFrost slides, air dried and placed in an X-ray cassette with BMR-2 film (Kodak) for 3 days. Following film development and confirmation of signals on autoradiographic films, slides were dipped in NTB2 photographic emulsion (Kodak) and stored in the dark at 4°C for 2 weeks. The slides were then developed with D-19 developer (Kodak) to precipitate the silver granules, stained with thionin label nucleus, dehydrated in graded ethanol solution, cleared with xylenes and cover-slipped with Permount mounting medium. The presence of cells labeled for GHSR mRNA was determined by the visualization of silver granules overlying the thionin-stained nuclei at 3x the background density of silver granule deposition.

4. Immunostainings. For fluorescent immunostaining, brain sections were treated with blocking solution (2% normal donkey serum and 0.25% Triton X-100 in PBS) and incubated with primary antibody (Supplementary Table 1) for 48 h at 4°C. Then, sections were incubated with secondary antibody for 2 h at room temperature (Supplementary Table 2). Finally, sections were mounted on glass slides and coverslipped with mounting media. For chromogenic immunostaining, brain sections were pretreated with 0.5% H_2O_2, treated with blocking solution and incubated with a primary antibody (Supplementary Table 1) for 48 h at 4°C. Then, sections were incubated with a biotinylated secondary antibody (Supplementary Table 2) for 1 h at room temperature and with avidin-peroxidase complex (Vectastain Elite ABC kit, Vector Laboratories, cat. PK6200) for 1 h, according to manufacturer's protocols. Then, visible signal was developed with 3-3′-diaminobenzidine (DAB, Sigma Aldrich, cat. D8001), giving a brown precipitate that was only observed in

labeled cells. Afterwards, sections were mounted on glass slides and coverslipped with mounting media. For double c-Fos/orexin, c-Fos/tyrosine hydroxylase (TH) or c-Fos/eGFP chromogenic immunostaining, brain sections of WT (for c-Fos/orexin or c-Fos/TH) or $GHSR^{eGFP}$ (for c-Fos/eGFP) mice were immunostained for c-Fos as described above but the signal was developed with DAB/nickel in order to have a black nuclear precipitate in c-Fos+ cells. Next, c-Fos immunostained sections were used for a second chromogenic staining using another primary antibody (anti-orexin, anti-TH or anti-eGFP) and developing the immunoreactive signal with DAB without nickel in order to produce a brown cytoplasmatic precipitate in cells positive for orexin, TH or eGFP.

5. Neuroanatomical analysis of eGFP+ cells in the LHA of $GHSR^{eGFP}$ mice. The distribution and the number of eGFP+ cells in the LHA were evaluated in a series of brain sections of $GHSR^{eGFP}$ mice (n=15) subjected to chromogenic immunostaining against eGFP. In addition, four series of brain sections of $GHSR^{eGFP}$ mice (n=2) were processed for chromogenic immunostaining against eGFP. In this case, each series was separately mounted, and microphotographed. Imaging was performed at low magnification, to capture the neuroanatomical landmarks, and at intermediate magnification to resolve cellular distribution within the LHA. Images were flat-field corrected and assembled into low and intermediate magnification mosaics using Fiji. For analysis, low magnification mosaics were sequentially loaded into trakEM2, following their original rostro-caudal order [41]. Then, intermediate magnification mosaics were registered within each section, producing a complete 3D volume of a hypothalamic segment containing the entire LHA. Afterwards, the LHA was delineated using the Allen Mouse Brain Atlas and the position of each eGFP+ cell within the LHA was manually annotated. In order to estimate the total number of LHA^{eGFP+} cells, all cells containing brown cytoplasmic staining were quantified. The spatial distribution of LHA^{eGFP+} cells was inspected for 3D clustering patterns using the DBSCAN algorithm [42] implemented in Fiji as a macro. Algorithm parameters used for the clustering were minPts=4 and Eps=60 μm, based on the analysis of the distribution of n-distances and preliminary scans. All delineated structures and cells were exported as 3D models and imported into Blender (http://www.blender.org/) for volumetric rendering. In order to compare if the spatial distribution of LHA^{eGFP+} cells was conserved between both $GHSR^{eGFP}$ mice, images containing the LHA^{eGFP+} cells each mouse were imported into DeepSlice to aligned the slices in the Allen Mouse Brain Common Coordinate Framework [43], which allows to adjust

the antero-posterior position, angle, rotation and scale of the images. Next, aligned data sets were mapped in Fiji using a brain-surface shape descriptor from Allen Mouse Brain Atlas to compare them in the same anatomic coordinate system.

6. Dual-label ISHH and immunostaining against eGFP or orexin. Brains sections in of $GHSR^{eGFP}$ mice or WT mice were subjected sequentially to ISHH against GHSR mRNA and next immunostaining against eGFP or orexin, respectively, using the procedures described above and as previously reported in detail [28]. The criteria used to determine if an LHA^{eGFP+} or $LHA^{orexin+}$ cell expressed GHSR mRNA was visualization of silver granules overlying the brown DAB precipitate at 3x the background density of silver granule deposition, which was estimated in a brain region known to lack GHSR expression.

7. Effect of intra-LHA injected ghrelin on mouse behavior. For intra-LHA treatment, mice were first stereotaxically implanted with a double indwelling bilateral guide cannula (Plastics One) above the LHA. Placement coordinates were: 1) antero-posterior: -1.58 mm, which is centered in the antero-posterior axis of the LHA, 2) lateral: ±1.0 mm, and 3) ventral: -2.50 mm. The location of the injectors avoids LHA damage and allows the diffusion of injected ghrelin into both LHA. After surgery, mice were individually housed (home cages: 19 x 28 x 13 cm), allowed to recover and accustomed to handling by removal of the dummy cannula for 5 days before experiments. On the test day, mice were intra-LHA injected with 0.2 µL of vehicle (artificial cerebrospinal fluid (aCSF) containing FluoSpheres 0.25% (Red Fluorescent, Invitrogen, cat# F8793) with or without 30 pmol/side of ghrelin (Global Peptides, cat. PI-G-03). Each mouse was used for a single assessment of either food intake or exploratory activity, and for two assessments of oxygen consumption, in a cross over fashion (see below). The accuracy of LHA injections was verified post-mortem. Only mice with visible bilateral tracts of injectors ~500 µm above the LHA and FluoSpheres observed exclusively in the LHA were included in the analysis. All testing was conducted during between 10:00 am and 2:00 pm.

Food intake assessment. Initially, food pellets were removed from the cage hoppers and the bedding was confirmed to be free of chow remains. Intra-LHA-injected mice were exposed to a pre-weighed chow pellet (~1500 mg) on the floor of the home cage. At 30-, 60- and 120-min posttreatment, chow pellets were collected and weighed in a calibrated scale with 1 mg precision. Food intake was calculated subtracting the remaining weight to the initial weight of pellets, and expressed in mg. Food intake was assessed in three

experiments testing: a) WT mice intra-LHA injected with vehicle (n=5) or ghrelin (n=6); b) ARH-intact and ARH-ablated mice intra-LHA injected with vehicle (n=4 and 5, respectively) or ghrelin (n=4 and 6, respectively); and c) NPY^{hrGFP} mice pretreated with the orexin 1 receptor antagonist SB-334867 (5 mg/g BW Tocris, cat. 1960, IP) and 30 min later intra-LHA injected with vehicle or ghrelin (vehicle/vehicle n=4, vehicle/ghrelin n=4, SB-334867/vehicle n=4, SB-334867/ghrelin n=6).

Activity assessment. Here, home cages were placed in a ventilated and acoustically isolated monitoring box (55 x 35 x 90 cm) equipped with an overhead camera and dimmable LED illumination. WT mice intra-LHA-injected with ghrelin (n=9) or vehicle (n=7) without access to food were recorded. Locomotor activity was assessed over 60 min and expressed in centimeters (cm). Exploratory behaviors were scored 10 min after intra-LHA injections and included rearing (standing on rear limbs), grooming (licking, scratching and nibbling), seeking and digging. Exploratory behaviors were expressed as the total time performing each behavior.

Oxygen consumption assessment. Here, WT mice (n=10) implanted with intra-LHA guide cannulas were place in the Oxyman/Comprehensive Lab Animal Monitoring System (CLAMS, Columbus Instruments, Columbus, OH, USA) for 3 days for acclimation. On the second- and third-days, mice were intra-LHA-injected with either vehicle and ghrelin, and oxygen consumption was continuously recorded for 60 min in mice that were kept without access to food. Oxygen consumption was estimated as the average of the 15-min time periods and expressed in ml/Kg/h.

8. Phenotypical characterization of eGFP+ neurons of the LHA of GHSR^{eGFP} mice. These analyses were performed in: a) naïve GHSR^{eGFP} mice (n=6); b) GHSR^{eGFP} mice that had been intracerebroventricularly (ICV) pretreated with colchicine (16 µg/mouse) 48-h before perfusion (n=7) and c) GHSR^{eGFP}/Gad2^{tdTomato} mice (n=3). All brain sections were used for fluorescent immunostaining against eGFP using a goat anti-eGFP antibody and a green secondary antibody, as described above. Next, sections of naïve GHSR^{eGFP} mice were used for red fluorescent immunostaining using either anti-neuronal nitric oxide synthase (anti-nNOS), anti-melanin concentrating hormone (anti-MCH) or anti-parvalbumin (see Supplementary Table 1 for details). Sections of colchicine-treated GHSR^{eGFP} mice were used for red fluorescent immunostaining using either anti-neurotensin, anti-somatostatin, anti-oxytocin, anti-thyrotropin-releasing hormone (anti-TRH) or anti-galanin antibodies (see Supplementary Table 1 for details). Sections of GHSR^{eGFP}/Gad2^{tdTomato}

mice were immunostained only against eGFP. Brain sections were sequentially mounted on glass slides, cover-slipped with mounting media containing Hoechst and used to acquire fluorescent images of the LHA. For each LHA, the total number of eGFP+ and/or red fluorescent cells were quantified. Results were expressed as a percentage, which represents cells positive for both eGFP and a given red signal as compared to the total number of eGFP+ cells.

9. Responsiveness of LHA neurons to systemic or central ghrelin treatments. For systemic treatment, mice were subcutaneously- (SC) injected with PBS alone (n=3) or containing 600 pmol/g BW of ghrelin (n=4), dose that elevates plasma ghrelin levels to concentrations reached under calorie restriction and increases food intake [44]. For central treatment, a single-indwelling guide cannula (Plastics One) was stereotaxically implanted into the lateral ventricle, as described in the past [45], one week before the study. Placement coordinates were: antero-posterior: −0.34 mm; lateral: ±1 mm and ventral: −2.3 mm. Here, mice were ICV-injected with 2µl of aCSF alone (n=3) or containing 300 pmol/mouse of ghrelin (n=6). All mice were perfused 2 h after treatment, and brain sections were obtained as described above and used for double c-Fos/eGFP immunostaining. Correct location of ICV cannula injectors was verified at the end of the experiment by histological analysis.

10. Labeling with fluorescent ghrelin (Fr-ghrelin). Fr-ghrelin is a variant of ghrelin conjugated to DY-647P fluorophore through a C-terminal Cys, which we have reported in the past [46]. For systemic administration, WT mice were SC-injected with vehicle alone (n=4) or containing 1200 pmol/g BW of Fr-ghrelin (n=3). For central administration, mice were ICV-injected with 2 µl of vehicle alone (n=3) or containing 60 pmol/mouse of Fr-ghrelin (n=6). The chosen dose of Fr-ghrelin are the minimum amounts of tracer that can be directly visualized in the mouse brain [46]. Mice were perfused at 15 min after treatment, and their brains were processed to generate coronal brain sections, as described above.

11. Calorie restriction protocol. $GHSR^{eGFP}$ mice were kept *ad libitum* fed (n=4) or calorie restricted for 5 days (n=7). For calorie restriction, body weight and overnight food intake of a subset of mice were initially daily monitored. Then, mice were fed with 40% of their daily food intake for 5 consecutive days at 11:00 h. Between 9:00 h and 11:00 h of the sixth day, calorie restricted mice were perfused, and brain sections used for c-Fos/eGFP immunostaining as described above.

12. Images acquisition and neuroanatomical analysis. Sections used for ISHH and/or chromogenic immunostaining were photographed with a bright-field Nikon Eclipse 50i microscope and a DS-Ri1 Nikon digital camera with a 0.45× adapter using 10×/0.3 and 40×/0.95 objectives. Sections used for fluorescent labeling were photographed using a Zeiss AxioObserver D1 equipped with an Apotome.2 structured illumination module, an AxioCam 506 monochrome camera, and 10×/0.45 and 40×/0.95 objectives. Emission filters were 400-550 nm for Alexa Fluor 488 (excitation 450-490 nm), 665-715 nm for Fr-ghrelin (excitation 625-655 nm), 570-640 nm for Alexa Fluor 594 or TdTomato (excitation 533-558 nm) and 420-470 nm for Hoechst (excitation 335-383 nm). All images were taken under the same optical and light conditions and were loaded into Fiji software for analysis. Quantitative analyses were performed in sections from bregma −0.34 to −2.80 mm, which includes the entire LHA [47]. A mouse brain atlas [48] was used to identify the anatomical limits of the LHA. All quantifications were bilaterally performed and corrected for double counting, according to Abercrombie's method [49], where the ratio of the actual number of cells to the observed number is represented by T/(T+h) where T=section thickness, and h=mean diameter of cells. For this, eGFP+ cell diameter of at least 30 cells was quantified using Fiji.

13. Statistical analyses. Normal distribution of data was tested using the D'Agostino & Pearson test. When a normal distribution was found, data were expressed as the mean ± standard error of the mean (SEM), and the experimental groups were compared with Student's unpaired t tests or one-way or two-way ANOVA, depending on the number of groups or experimental design. In this case, outliers were detected using the ROUT method and were excluded from the analysis (n=3). When a normal distribution was not found, data were expressed as median ± interquartile range and compared with the non-parametric Mann-Whitney or Kruskal-Wallis test. Tests used for each comparison are indicated in each figure legends. Differences were considered statistically significant when $p<0.05$. Of note, no significant differences ($P > 0.09$) were observed in c-Fos induction in the ARH or the LHA between mice SC- or ICV-treated with vehicle and thus the data were pooled and termed the vehicle-treated group. Statistical analyses were conducted using GraphPad Prism 9.0.

RESULTS

Neuroanatomical analysis of LHA^{GHSR} neurons. Our ISHH experiments using a probe against GHSR mRNA as well as the analysis of ISHH data reported by the Allen Mouse Brain Atlas [50] revealed the presence of LHA^{GHSR} cells in brain sections of WT mice **(Figure 1A-B)**. Immunostaining against eGFP in brain sections of GHSR^{eGFP} mice also revealed the presence of LHA^{eGFP+} cells **(Figure 1C)**. In order to test if the GHSR^{eGFP} mouse line was an accurate reporter model to study LHA^{GHSR} cells, we performed ISHH to identify LHA^{GHSR} cells and brown chromogenic immunostaining to visualize LHA^{eGFP+} cells in GHSR^{eGFP} mice **(Figure 1D)**. The quantitative analysis indicated that LHA^{GHSR}/LHA^{eGFP} cells represented 78±5 % of the total LHA^{eGFP+} cells. Thus, GHSR^{eGFP} mice are an accurate tool to investigate LHA^{GHSR} neurons. Then, another set of brain sections of GHSR^{eGFP} mice was used for a chromogenic staining against eGFP and a detailed neuroanatomical analysis of the distribution and cytoarchitectonic features of LHA^{eGFP+} cells throughout the rostro-caudal axis of the nucleus. Most LHA^{eGFP+} cells displayed an ovoid soma of 10±0.2 µm of diameter and two or three short sparsely branched fibers, independently of the rostro-caudal level **(Figure 1E)**. The quantitative analysis revealed the presence of a total of 815±177 LHA^{eGFP+} cells per mouse **(Figure 1F)**. In order to gain more insights about the distribution of the LHA^{eGFP+} cells, we computationally mapped their position. For this, we aligned and performed a 3D reconstruction of a complete series of brain sections and, after that, extracted the localization of the LHA^{eGFP+} cells from the images **(Figure 2A-D)**. The analysis of 3D distribution of LHA^{eGFP+} cells indicated that they are homogeneously distributed within the LHA. As we have done in the past [45], we also performed a clustering analysis on LHA^{eGFP+} cell coordinates using the DBSCAN algorithm and could not find evidence of distinct clusters of LHA^{eGFP+} cells. Of note, we performed an additional 3D map of the distribution of the LHA^{eGFP+} cells within another GHSR^{eGFP} mouse and found similar results **(Supp Figure 1)**.

Ghrelin action in the LHA. Next, we investigated the physiological implications of the local bilateral action of ghrelin in the LHA **(Figure 3A)**. In mice with access to food, intra-LHA-injected ghrelin induced a transient ~10-fold increase of food intake at 30-min post-treatment (**Figure 3B).** In mice without access to food, intra-LHA-injected ghrelin induced a transient increase of locomotor activity **(Figure 3C)**. In contrast, intra-LHA-injected ghrelin

did not affect digging, rearing, jumping or grooming behaviors nor oxygen consumption **(Figure 3D-H)**.

Neuronal circuit mediating the orexigenic actions of ghrelin in the LHA. In order to clarify the brain targets recruited by ghrelin action in the LHA, we assessed c-Fos in brain regions heavily innervated by LHA neurons of mice intra-LHA-injected with ghrelin or vehicle. Here, we performed a double immunostaining against c-Fos, which was visualized as a black purple precipitate (c-Fos+), and TH, which was visualized as a brown precipitate (TH+) and used to identify dopamine neurons of the VTA that are a known target of LHA neurons [51]. We found that intra-LHA-injected ghrelin induced a ~2-fold increase of the number of c-Fos+ cells in the ARH, as compared to intra-LHA-injected vehicle (54±11 vs. 25±5 c-Fos+ cells/slice respectively, unpaired t-test, p=0.04), whereas it did not affect the number of c-Fos+ cells in LHA (see below), the nucleus accumbens (Acb), the VTA, the bed nucleus of the stria terminalis (BNST), the hypothalamic paraventricular nucleus (PVH), the lateral habenula (LHb), the thalamic paraventricular nucleus (PVT) or the central amygdala (CeA) **(Figure 4A-H)**. Also, intra-LHA-injected ghrelin did not affect the fraction of c-Fos+/TH+ cells in any brain area, as compared to intra-LHA-injected vehicle (not shown).

In order to test whether the acute orexigenic effect of intra-LHA-injected ghrelin requires the ARH, we assessed if intra-LHA-injected ghrelin affects food intake in ARH-ablated mice (**Figure 5A)**. Here, we found a significant interaction between model and treatment indicating that food intake response to intra-LHA-injected ghrelin depended on the mouse model. In particular, intra-LHA-injected ghrelin increased food intake in ARH-intact mice, but not in ARH-ablated mice (**Figure 5A)**. Thus, the orexigenic effect of intra-LHA-injected ghrelin requires the integrity of the ARH.

In rats, ICV-injected ghrelin has been shown to activate LHA^{orexin} cells, which mediate orexigenic responses [30]. Thus, we assessed if LHA^{orexin} cells are activated in mice intra-LHA-injected with ghrelin, and found that intra-LHA-injected ghrelin increased the fraction of LHA^{orexin} positive for c-Fos+, as compared to mice intra-LHA-injected with vehicle (6±1 vs. 1±0 % of c-Fos+/orexin+ cells, respectively, **Figure 6A**). Previous evidence showed that the orexigenic effect of the LHA^{orexin} neurons involves the $ARH^{NPY/AgRP}$ neurons (see discussion section). Since we found that the ARH is required for the orexigenic effect of intra-LHA-injected ghrelin, we assessed if an intra-LHA injection of ghrelin induces c-Fos

expression in hrGFP+ neurons of the ARH of NPY^{hrGFP} mice. We found that intra-LHA-injected ghrelin increased the fraction of ARH$^{NPY/AgRP}$ neurons positive for c-Fos+, as compared to mice intra-LHA-injected with vehicle (**Figure 6B and D**). In order to determine if orexin receptor 1 signaling was required for the orexigenic effect of intra-LHA-injected ghrelin, we treated NPY^{hrGFP} mice with the orexin receptor 1 antagonist SB-334867 and subsequently intra-LHA-injected ghrelin or vehicle. Here, food intake and c-Fos responses showed significant interaction between pretreatment and intra-LHA injections. In particular, SB-334867 pretreatment reduced food intake (**Figure 6C**) and the fraction of ARH$^{NPY/AgRP}$ neurons positive for c-Fos+ (**Figure 6D**) in mice that were intra-LHA-injected with ghrelin, as compared to vehicle-pretreated mice and intra-LHA-injected with ghrelin. Thus, ghrelin's action in the LHA involves the recruitment of LHA^{orexin} neurons that, in turn, activate the ARH$^{NPY/AgRP}$ neurons.

Phenotypical analysis of LHA^{GHSR} neurons. Next, we wondered if GHSR is present in LHA^{orexin} neurons, and performed red fluorescent immuno-staining against orexin in brain sections of GHSR^{eGFP} mice. We found no double labeled LHA^{eGFP+} cells and LHA^{orexin} cells (**Figure 7A**). As an alternative strategy, we performed ISHH against GHSR mRNA and immuno-staining against orexin in brain samples of WT mice, and again we did not find cells positive for both signals (**Figure 7B**). In order to determine the neurochemical phenotype of the LHA^{eGFP+} cells, we performed red fluorescent immuno-staining against specific markers for different neuronal types. In brain sections of naïve GHSR^{eGFP} mice, we found that 8±1% of LHA^{eGFP+} cells were nNOS+ (**Figure 7C**) but they were not positive for MCH, parvalbumin or oxytocin **(Figure 7D-F)**. In brain sections of colchicine-treated GHSR^{eGFP} mice, we found that 2±1% of LHA^{eGFP+} cells were neurotensin+ **(Figure 7G**) but were not positive for somatostatin, TRH or galanin **(Figure 7H-J)**. Also, we studied GHSR^{eGFP}/Gad2^{tdTomato} mice, and we found that LHA^{eGFP+} cells did not co-localize with tdTomato+ cells **(Figure 7K)**.

Analysis of the responsiveness of LHA^{GHSR} neurons to plasma ghrelin. In order to test if LHA^{GHSR} cells respond to circulating or CSF ghrelin, we SC- or ICV-injected GHSR^{eGFP} mice with ghrelin, or vehicle, and assessed c-Fos induction in LHA^{eGFP+} cells **(Figure 8A)**. As expected, we confirmed that the number of c-Fos+ increased in the ARH of mice SC- or ICV-injected with ghrelin, as compared in vehicle-treated mice [32]. Also, the fraction of LHA^{eGFP+} cells positive for c-Fos increased in GHSR^{eGFP} mice ICV-injected with

ghrelin, as compared to the $GHSR^{eGFP}$ mice treated with vehicle, but was unaffected in $GHSR^{eGFP}$ mice SC-injected with ghrelin (30±9, 2±1 and 4±2 % of LHA^{eGFP+} positive for c-Fos as compared to total LHA^{eGFP+} cells, respectively).

In order to test if LHA^{GHSR} neurons are reached by plasma or CSF ghrelin, we SC- or ICV-injected WT mice with Fr-ghrelin, or vehicle, and looked for Fr-ghrelin signal in the LHA and the ARH, which is accessible to ghrelin present in plasma or CSF **(Figure 8B)**. As expected, we confirmed the presence of Fr-ghrelin signal in cells in the ARH of mice SC- or ICV-injected with Fr-ghrelin, as we found in the past [32, 46]. Conversely, we did not find cells positive for Fr-ghrelin in the LHA of mice injected with the fluorescent analog. Indeed, the fluorescence signal in the LHA of mice SC- or ICV-injected with Fr-ghrelin did not differ from the signal found in vehicle-treated mice (1.0±0.1, 1.1±0.1 and 1.0±0.1 fluorescent intensity a.u., respectively).

Finally, we assessed if LHA^{GHSR} neurons show c-Fos induction in response to elevations of endogenous ghrelin, and for this purpose investigated calorie restricted $GHSR^{eGFP}$ mice **(Figure 8C)**, which display a ~9.3-fold increase in plasma ghrelin levels, as compared as *ad libitum* fed mice [15]. The quantitative analysis indicated that the total number of LHA^{eGFP+} cells (not shown) as well as the fraction of LHA^{eGFP+} cells positive for c-Fos+ did not differ between calorie restricted and *ad libitum* fed $GHSR^{eGFP}$ mice (1.0±0.4 and 2±1% LHA^{eGFP+} cells positive for c-Fos as compared to all LHA^{eGFP+} cells, respectively).

DISCUSSION

Here, we provide a neuroanatomical and functional characterization of the LHA^{GHSR} neurons in male mice. We report that: 1) LHA^{GHSR} neurons are homogeneously distributed throughout the entire nucleus; 2) intra-LHA injections of ghrelin transiently increase food intake and locomotor activity; 3) ghrelin's orexigenic effect in the LHA involves the indirectly recruitment of LHA^{orexin} neurons and $ARH^{NPY/AgRP}$ neurons; and 4) LHA^{GHSR} neurons are not targeted by plasma or CSF ghrelin. Based on our observations, we propose a hypothetical model of the circuit mediating the ghrelin's orexigenic effects in the LHA **(Figure 9)**. Thus, LHA^{GHSR} cells are part of a hypothalamic neuronal circuit that potently induces food intake, and whose physiological implications remain to be elucidated.

GHSR-expressing cells are present in the mouse LHA, as detected by ISHH. LHA^{GHSR} cells were also clearly visualized in $GHSR^{eGFP}$ mice, which was an accurate animal model to investigate them since the double eGFP protein and GHSR mRNA labeling indicated that ~80% of LHA^{eGFP} cells express GHSR mRNA. Since LHA^{GHSR} cells are unambiguously and reproducibly labeled in $GHSR^{eGFP}$ mice, we estimated its number and neuroanatomical distribution in the reporter animals. According to our estimations, ~800 LHA^{GHSR} cells exist in the mouse brain, a number that is likely physiologically relevant and may affect animal's behaviors given that a previous report showed that the optogenetic activation of ~800 $ARH^{NPY/AgRP}$ neurons is sufficient to trigger voracious food intake in mice [52]. LHA^{GHSR} cells were found sparsely distributed within the entire nucleus and lacked any evident cluster organization, in contrast to our observations for GHSR-expressing cells in other brain areas [16]. Chromogenic staining against eGFP in brain sections of $GHSR^{eGFP}$ mice also allowed us to visualize the morphology of LHA^{GHSR} cells. The finding that most LHA^{GHSR} cells displayed similar cytoarchitectonic features suggests that they represent a functionally unique subset of cells. Also, the observation that LHA^{GHSR} cells have fibers in the coronal plane suggests that they could be neurons involved in local circuits of the LHA, which are particularly important in this brain area [53].

We found here that intra-LHA injections of ghrelin transiently evoke food intake in mice, as previously shown in rats [18, 29, 54, 55]. The robust feeding response (e.i., ~10-fold) and the relatively small dose of ghrelin used in the study (30 pmol/side, as compared

to 300 pmol/side used in some of the above referred rat studies) indicate that ghrelin's orexigenic effect in the mouse LHA is very potent. The observations that intra-LHA-injected ghrelin did not affect digging, rearing, jumping or grooming behaviors indicate that ghrelin's orexigenic effect in the LHA is selective, whereas the finding that intra-LHA-injected ghrelin did not affect oxygen consumption agrees previous findings in using centrally-injected ghrelin in rats [56, 57] or mice [3]. Of note, we cannot rule out that ghrelin's effect in the LHA is, in part, due to the action of the hormone on GHSR located in terminals of neurons innervating the LHA, as shown in other brain areas [44, 58, 59]. For instance, GHSR-expressing glutamatergic neurons of the ventral hippocampus were shown to drive food intake via direct innervation and activation of the LHA^{orexin} neurons [60], although it remains to be assessed if GHSR is present in the terminal ends of these hippocampal neurons.

Current study clarifies the neurobiological basis mediating ghrelin's orexigenic effect in the LHA. First, the neuroanatomical mapping of c-Fos induction highlighted a role of the ARH as a downstream target of ghrelin action in the LHA. Second, the observation that intra-LHA-injected ghrelin did not induce feeding in ARH-ablated mice indicated that the ARH is required for such ghrelin's orexigenic effect. Third, intra-LHA-injected ghrelin resulted in the induction of c-Fos in LHA^{orexin} neurons and $ARH^{NPY/AgRP}$ neurons, which are known to potently increase food intake [52]. Notably, GHSR was not expressed in LHA^{orexin} neurons, but the pharmacological blockage of orexin 1 receptor in mice intra-LHA-injected with ghrelin fully blocked the ghrelin-induced food intake and c-Fos induction in the $ARH^{NPY/AgRP}$ neurons. Since it has been shown that LHA^{orexin} neurons densely innervate the ARH [61] and that centrally-injected orexin A induces both activation of the $ARH^{NPY/AgRP}$ neurons and food intake acting via the orexin 1 receptor [62–64], it seems reasonable to hypothesize that intra-LHA-injected ghrelin acts on LHA^{GHSR} neurons and, via a still unknown mechanism, activates the LHA^{orexin} neurons that further recruit $ARH^{NPY/AgRP}$ neurons to induce feeding. Of note, the fact that blocking the orexin 1 receptor signaling blocked c-Fos induction in the $ARH^{NPY/AgRP}$ of mice intra-LHA-injected with ghrelin underestimate the possibility that ghrelin's orexigenic effect in the LHA involves the action of the hormone on GHSR located in terminal ends of $ARH^{NPY/AgRP}$ neurons, which heavily innervate the LHA (PMID: 9862320). Still, future studies are required to clarify the intricacies that mediate the ARH and LHA crosstalk.

We unexpectedly found that GHSR is not expressed in LHA^{orexin} neurons of mice, using two different experimental strategies (i.e., ISHH against GHSR and immunostaining against orexin in WT mice or double immunostaining against orexin and eGFP in GHSR^{eGFP} mice). Our observation is in line with a recent single-cell expression profiling analysis showing that LHA^{orexin} neurons do not express GHSR in mice [65]. Of note, an early report showed that ghrelin depolarizes and increases firing frequency in 6-out-9 isolated LHA^{orexin} neurons of a reporter mouse model [66], such small number of assessed cells, of a total of ~2800 orexin neurons in mice [67], and the differences in the experimental approaches make difficult to identify the reasons behind the apparent discrepancy. Our observation that ghrelin indirectly recruits LHA^{orexin} neurons via an intra-LHA circuit is rather in line with the notion that the activity of LHA^{orexin} neurons is tightly regulated by local neurons [68].

We found that LHA^{GHSR} cells do not express MCH, parvalbumin, somatostatin, oxytocin, TRH or galanin, some of which could have mediated local ghrelin-induced activation of LHA^{orexin} neurons [68]. Also, we found that LHA^{GHSR} cells are not GABA cells, based on the observations in the GHSR$^{eGFP/}$Gad2^{tdTomato} mice. However, we cannot rule out that GHSR is expressed in a different subset of LHA^{GABA} neurons, such as the ones expressing the Gad1 isoform [69]. Interestingly, we found that ~8% of LHA^{GHSR} neurons express nNOS, which produce nitric oxide that acts locally inhibiting LHA^{orexin} neurons [70]. Thus, it is possible that ghrelin's actions in the LHA may involve inhibition of local nNOS neurons. Also, we found that ~2 % of LHA^{GHSR} neurons express neurotensin. A previous study showed that ghrelin treatment does not induce c-Fos in LHA neurons producing neurotensin [67] that, indeed, is an anorectic neuropeptide [71]. Thus, ghrelin's actions in the LHA likely do not involve local neurotensin neurons. Despite our efforts, the neurochemical identity of most LHA^{GHSR} neurons remains to be elucidated. In this regard, a potential target of ghrelin in the LHA may be glutamatergic neurons, which are present in the LHA, are known to potently activate LHA^{orexin} neurons and play important local roles [53, 68]. Thus, future studies will be necessary to test if ghrelin targets local LHA glutamatergic neurons that, in turn, regulate LHA^{orexin} neurons.

We found here that intra-LHA injections of ghrelin transiently increase locomotor activity in mice, which is a functional indication that ghrelin stimulates LHA neurons since electrical stimulation of the LHA is known to induce "stepping" in anaesthetized rats [72, 73].

The neurobiological basis mediating the locomotor effect of intra-LHA-injected ghrelin were not addressed here, but they may involve the recruitment of the mesolimbic pathway since intra-LHA-injected ghrelin was shown to potentiate dopamine spikes in the Acb [54]. Also, it is likely that the locomotor effect of intra-LHA-injected ghrelin involves the LHA^{orexin} neurons since they innervate multiple brain areas that drive or modulate locomotion, including the substantia nigra, VTA, Acb, motor cortex, locus coeruleus, and spinal cord [61, 74, 75], and its optogenetic activation induces running [76]. Of note, we did not detect c-Fos induction in response to intra-LHA injection of ghrelin in some of the above referred brain areas associated to locomotion; however, c-Fos is not an ideal marker for these mesolimbic structures as most of them show weak c-Fos labeling when activated [16]. Finally, it is important to highlight that intra-LHA injected ghrelin was shown to promote wakefulness in rats [55]. Thus, the extent to which the effects of intra-LHA-injected ghrelin on food intake and locomotor activity are affected by the arousal state are uncertain. In any case, the intricacies regarding LHA's roles in modulation of the referred behavioral outputs are very hard, if possible, to dissociate [77].

Current studies using bolus injections of a fluorescent analog of ghrelin indicate that ghrelin present in plasma or CSF do not acutely reach the LHA. These observations are in line with a number of studies from our team [78–80], and other research groups [81], indicating that rapid elevations of circulating ghrelin do not directly impact in brain areas distantly located from the fenestrated capillaries and brain ventricles in mice. In line with the notion that plasma ghrelin does not reach the LHA^{GHSR} neurons, LHA^{eGFP} cells did not show a c-Fos induction in calorie-restricted $GHSR^{eGFP}$ mice, in which plasma ghrelin is highly increased. Of note, current imaging studies were performed using a fluorescent version of ghrelin labeled with DY-647P, a far-red fluorophore that is directly visualized in the samples. In the past, we assessed the accessibility of ghrelin to different mouse brain areas, including the LHA, using fluorescein-labeled ghrelin, that can be visualized at lower levels using a chromogenic immunostaining against fluorescein [32, 82]. In our previous study, we concluded that centrally-injected, but not systemically-injected, fluorescein-labeled ghrelin could reach the LHA [32]. However, the current study, in which the LHA was more precisely delimited and lower doses of fluorescent ghrelin were centrally injected used, indicates that even centrally-injected ghrelin cannot access into the LHA. Of note, we found that ~10% of LHA^{GHSR} neurons increased c-Fos expression in response to centrally-injected ghrelin, but this activation could take place via indirect mechanisms. In any case, ghrelin is not produced

in the mouse brain [83] and is undetectable in the mouse aCSF [46]. Thus, it seems more likely that GHSR in the LHA plays ghrelin-independent actions that may depend on its constitutive activity, its capability to regulate other G protein coupled receptors or its recently recognized role as a receptor for liver-expressed antimicrobial peptide 2 [84, 85].

Here we clarify the neurobiological basis by which ghrelin acts in the LHA and regulates food intake in male mice. Intriguingly, the orexigenic effect of ghrelin is more potent in males than in females, in both rats and mice [86, 87]. Also, it was reported that intra-LHA-injected ghrelin more potently increases food intake in male rats than in female rats, whereas it only induces food seeking behaviors in female rats [17]. In light of this previous report, future studies should be performed to investigate the neurobiological basis mediating the putative sexually dimorphic roles of the LHA^{GHSR} neurons. Hopefully, a better understanding of the orexigenic actions of ghrelin in the LHA would help to develop newer pharmacological strategies to increase appetite is some human conditions.

ACKNOWLEDGEMENTS

This work was supported by grants from Fondo para la Investigación Científica y Tecnológica (FONCyT, PICT2017-3196, PICT2019-3054 and PICT2020-3270 to MP), The National Qatar Research Foundation (NPRP13S-0209-200315 to MP). We would like to thank to Dr. A. Abizaid (Carleton University), Dr. J. Belforte (University of Buenos Aires), Dr. E Nillni (Brown University), Dr. A. Mecawi (Universidade Federal de São Paulo), Dr. H. Munzberg (Luisiana State University), Dr. A. Schinder (Leloir Institute) for providing the antibodies against neurotensin, parvalbumin, TRH, oxytocin, galanin and somatostatin respectively. Also, we would also like to thank to Dr. M.J. Tolosa, Dr. G. García-Romero, and Ms. B. Cudazzo for the technical assistance and to Dr. M. P. Cornejo for her discussion about the project.

FIGURE LEGENDS

Figure 1. Neuroanatomical analysis of LHA^{GHSR} neurons. A-D display representative images of coronal brain slices containing a set of hypothalamic regions including the LHA. Each panel shows GHSR-expressing cells through diverse techniques: A. ISHH against GHSR-mRNA in WT mice. B. ISHH against GHSR-mRNA in WT mice. This image was obtained from the Allen Mouse Brain Atlas. C. Immunofluorescence against eGFP in GHSR^{eGFP} mice. D. ISHH against GHSR-mRNA and immunostaining against eGFP in GHSR^{eGFP} mice. **E** display three representative high magnification images of LHA^{eGFP+} cells with two or three branched fibers, obtained from GHSR^{eGFP} mice. **F** display a bar graph indicating a quantitative analysis of the number of eGFP+ cells along the LHA-rostro-caudal axis of GHSR^{eGFP} mice. Data is presented as mean ± SEM. In all cases, the wedges in the images indicate LHA^{GHSR+} cells detected by each methodology. Inserts display high magnification images taken from the areas indicated in low magnification photomicrographs. Scale bar: low magnification, 100 μm; high magnification 10 μm.

Figure 2. **Spatial reconstruction of LHA^{eGFP+} cells in GHSR^{eGFP} mice**. The figure displays representative projection of all eGFP+ cells found in 54 serial section of GHSR^{eGFP} mouse. **A-D** shows different 3D-renderings of the LHA^{eGFP+} cells, and surrounding structures. **A** and **B** displays a fronto-lateral view. **C** and **D** displays a frontal orthogonal view and a dorsal orthogonal view, respectively. The insets in B-D provide a wider view of each rendering. A, anterior, P posterior, D dorsal, V ventral, L left, R right, cc corpus callosum, fx fornix, mt mammillothalamic tracts, v ventricles system, opt optic tracts, LHA^{eGFP+} cells.

Figure 3. Intra-LHA-injected ghrelin transiently increases food intake and locomotor activity. **A** displays representative images of a brain section belonging to a mouse subjected to an intra-LHA cannulation. The left image shows a schematic representation of the placement of the guide cannula and the internal cannula in a coronal brain section including the LHA. The right image shows a brain section including the trace of the internal cannula indicated by the punctuated red rectangles. **B** displays the quantitative analysis of the food intake induced by the injection of vehicle (n=5) or ghrelin (n=6) intra-LHA along 2-h after injection. Two-way ANOVA [$F_{int(}2,27)=3.598$ $p=0.0412$, $F_{time}(2,27)=3.078$ $p=0.0623$, $F_{treatment}(1,27)=10.41$ $p=0.0033$] followed by Tukey´s multiple comparisons test (**, $p < 0.01$ vs. vehicle intra-LHA). **C** displays the quantitative analysis of the distance travelled induced

by the injection of vehicle (n=7) or ghrelin (n=9) intra-LHA along 30 min after the injection. Two-way ANOVA [$F_{int}(30,420)=2.070$ p=0.0010, $F_{time}(30,420)=11.70$ p<0.0001, $F_{treatment}(1,14)=1.483$ p=0.2435] followed by Tukey´s multiple comparisons test (**, p< 0.01 vs. vehicle intra-LHA). In this case, the graph displays only the first 15 min of activity after the injection. **D-G** indicate the quantitative analysis of the time that mice display digging (D), rearing (E), jumping (F) and grooming (G) along 30 min after the injection. **H** displays the quantitative analysis of the energy expenditure (VO_2) of the mice along 30 min after the injection. In all cases data is presented as mean ± SEM.

Figure 4. Intra-LHA injected ghrelin increases c-Fos+ cells in the ARH nucleus. Displays representative images of different brain regions subjected to immunostaining against c-Fos (black) and TH (brown) proceeding from mice injected with vehicle (n=7) or ghrelin (n=9) intra-LHA. Inserts display high magnification images taken from the areas indicated in low magnification photomicrographs. Wedges point to TH+ cells and arrowheads point c-Fos+ cells. Unpaired t-test for the quantification of the c-Fos+ cells in the ARH [t(14)=2.175 p=0.0473]. Acb, accumbens, BNST, bed nucleus of the stria terminalis; PVH, paraventricular nucleus of the hypothalamus; LHb, lateral habenula; PVT, paraventricular nucleus of the thalamus; ARH, arcuate nucleus of the hypothalamus; CeA, central amygdala; VTA, ventral tegmental area. Scale bar: low magnification, 100 µm; high magnification 10 µm.

Figure 5. **The orexigenic effect of intra-LHA injected ghrelin is abrogated in ARH-ablated mice**. Bar graph displays the quantitative analysis of the total food consumed after 2 h of the ghrelin or vehicle intra-LHA injection in mice with the ARH-intact or the ARH-ablated. Data is presented as mean ± SEM. Two-way ANOVA [$F_{int}(1,15)=10.77$ p=0.0050, $F_{PBS/MSG}(1,15)=5.368$ p=0.0351, $F_{veh/ghr}(1,15)=19.67$ p=0.0005] followed by Tukey´s multiple comparisons test (**, p< 0.01; ***, p<0.001).

Figure 6. **Intra-LHA injected ghrelin induces c-Fos in LHA^{orexin} neurons and induces food intake and c-Fos in $ARH^{NPY/AgRP}$ neurons via an orexin 1 receptor mechanism**. **A** displays representative images of brain sections that include the LHA subjected to immunostaining against c-Fos (black) and orexin (brown) proceeding from WT mice injected with vehicle or ghrelin intra-LHA. Arrows point to c-Fos+/orexin+ cells, wedges point to orexin+ cells and arrowheads point to c-Fos+ cells. Unpaired t-test [t(14)=2.209 p=0.0443].

B displays representative images of brain sections that include the ARH subjected to immunostaining against c-Fos (purple) proceeding from NPY^{hrGFP} mice injected with vehicle or ghrelin intra-LHA. Arrows point to c-Fos+/hrGFP+ cells and wedges point to hrGFP+ cells. In all cases, insets display high magnification images taken from the areas indicated in low magnification photomicrographs. **C** displays the quantitative analysis of the total food consumed after 2 h of the vehicle or ghrelin intra-LHA injection in NPY^{hrGFP} mice IP preinjected with SB-334867 or vehicle. Two-way ANOVA [$F_{int}(1,14)=7.055$ p=0.0188, $F_{SB/Veh}(1,14)=12.72$ p=0.0031, $F_{veh/ghr}(1,14)=12.32$ p=0.0035] followed by Tukey´s multiple comparisons test (**, p< 0.01; ns, non-significative). **D** display the quantitative analysis of the fraction of hrGFP cells in the ARH nucleus of the NPY^{hrGFP} mice that are c-Fos-IR. Two-way ANOVA [$F_{int}(1,14)=9.089$ p=0.0093, $F_{veh/SB}(1,14)=8.005$ p=0.0134, $F_{veh/ghr}(1,14)=24.91$ p=0.0002] followed by Tukey´s multiple comparisons test (**, p< 0.01; ***, p<0.001; ns, non-significative). In all cases, data is presented as mean ± SEM. Scale bar: low magnification, 100 µm; high magnification 10 µm.

Figure 7. A fraction of LHA^{GHSR} cells are nNOS+ or neurotensin+. **A** displays immunostaining against eGFP and orexin in the LHA of $GHSR^{eGFP}$ mice. **B** displays an ISHH against GHSR-mRNA and immunostaining against orexin in the LHA of WT mice. **C-J** display immunostaining against eGFP and diverse neuropeptides in the LHA of $GHSR^{eGFP}$ mice including nNOS, MCH, parvalbumin, oxytocin, neurotensin, somatostatin, TRH and galanin respectively. **K** displays immunostaining against eGFP in $GHSR^{eGFP}/Gad2^{tdTomato}$ mice. Insets display high magnification images taken from the areas indicated in low magnification photomicrographs. Arrows indicate double IR-cells (eGFP+/nNOS+ or eGFP+/neurotensin+ cells), wedges indicate eGFP+ cells and arrowheads indicate positive cells for the different neurochemical markers. Scale bar: low magnification, 100 µm; high magnification 10 µm.

Figure 8. Circulating ghrelin do not induce c-Fos in LHA^{GHSR} cells and Fr-ghrelin do not reach the LHA. A display representative images of brain sections containing the LHA subjected to immunostaining against c-Fos and eGFP from $GHSR^{eGFP}$ mice systemically or ICV-injected with ghrelin or vehicle. Arrows indicate c-Fos+/eGFP+ cells, wedges indicate eGFP+ cells and arrowheads indicate c-Fos+ cells. Kruskal-Wallis test [H(3,13)=6.087 p=0.0206] followed by Dunn´s multiple comparisons test (p=0.0227 ICV-injected ghrelin vs. vehicle). **B** displays representative images if brain section containing the LHA and the ARH

from WT mice systemically or ICV-injected with Fr-ghrelin or vehicle. Wedges indicate Fr-ghrelin+ cells. One-way ANOVA [F(2,12)=0.7483 p=0.4940]. **C** display representative images of brain section containing the LHA subjected to immunostaining against c-Fos and eGFP from of $GHSR^{eGFP}$ mice exposed to calorie restriction or fed *ad libitum*. Unpaired t-test [t(9)=0.8666 p=0.4087]. Wedges indicate eGFP+ cells and arrowheads indicate c-Fos+ cells. In all cases, insets display high magnification images taken from the areas indicated in low magnification photomicrographs. Scale bar: low magnification, 100 μm; high magnification 10 μm.

Figure 9. **Hypothetical model of the neuronal circuit mediating the orexigenic effect of intra-LHA injected ghrelin**. Ghrelin action on LHA^{GHSR} neurons induce LHA^{orexin} activation which, in turn, activate $ARH^{NPY/AgRP}$ neurons inducing food intake.

SUPPLEMENTARY MATERIAL

Supplementary figure 1. Spatial disposition of LHA^{GHSR} cells is conserved in two different mouse brains. Figure display different 3D spatial renderings of the LHA^{eGFP+} cells belonging of two different mice. The LHA^{GHSR} cells from the different set of data are represented as yellow or light-green balls. **A** and **B** display a frontal and lateral orthogonal view respectively and **C** display a dorsal orthogonal view. Insets display a wider view of each rendering. A, anterior, P posterior, D dorsal, V ventral, L left, R right.

Supplementary table 1. Primary antibodies used, either for chromogenic (c) or fluorescent (f) immunostaining.

Antibody	Manufacturer, Catalog	Species Raised in	Dilution Used
Anti-eGFP	Molecular Probes, A-6455	Rabbit	1:5000 (c)
	Vector Lab., BA-0702	Goat	1:1000 (f)
Anti-c-Fos	Santa Cruz, SC-7202	Rabbit	1:20000 (c)
			1:2000 (f)
Anti-Orexin	Phoenix Pharm., H-003-30	Rabbit	1:20000 (c)
			1:10000 (f)
Anti-TH	Santa Cruz, SC-14007	Rabbit	1:20000 (c)
Anti-nNOS	Zymed Company, 61-7000	Rabbit	1:3000 (f)
Anti-MCH	Phoenix Pharm., H-070-47	Rabbit	1:2000 (f)
Anti-Parvalbumin	Swant, PV27	Rabbit	1:2000 (f)
Anti-Neurotensin	Immunostar, 20072	Rabbit	1:1000 (f)
Anti-Somatostatin	Sigma Aldrich, MAB354	Rat	1:250 (f)
Anti-Oxytocin	Dr. Harold Gainer (NIH, Bethesda, USA) [88]	Mouse	1:1000 (f)
Anti-TRH	Dr. Eduardo Nillni (Brown University, USA) [89]	Rabbit	1:1000 (f)
Anti-Galanin	Peninsula, T-4330	Rabbit	1:1000 (f)

Supplementary table 2. Secondary antibodies used.

Antibody	Manufacturer, Catalog	Species Raised in	Dilution Used
Biotinylated Anti-Rabbit	Vector Lab., BA-1000	Donkey	1:3000
Alexa Fluor594 Anti-Rat	Invitrogen, A-21209	Donkey	1:1000
Alexa Fluor594 Anti-Rabbit	Invitrogen, A-21207	Donkey	1:1000
Alexa Fluor594 Anti-Mouse	Molecular Probes, A21203	Donkey	1:1000
Alexa Fluor488 Anti-Goat	Life Technologies, A11055	Donkey	1:1000

REFERENCES

1. Müller TD, Nogueiras R, Andermann ML, et al (2015) Ghrelin. Mol Metab 4:437–460. https://doi.org/10.1016/j.molmet.2015.03.005

2. Garin MC, Burns CM, Kaul S, Cappola AR (2013) Clinical review: The human experience with ghrelin administration. J Clin Endocrinol Metab 98:1826–1837. https://doi.org/10.1210/jc.2012-4247

3. Cornejo MP, Denis RGP, García Romero G, et al (2021) Ghrelin treatment induces rapid and delayed increments of food intake: a heuristic model to explain ghrelin's orexigenic effects. Cell Mol Life Sci 78:6689–6708. https://doi.org/10.1007/s00018-021-03937-0

4. Mn K, A G, S G, Zs Q (2018) Ghrelin as a Promising Therapeutic Option for Cancer Cachexia. Cellular physiology and biochemistry : international journal of experimental cellular physiology, biochemistry, and pharmacology 48:. https://doi.org/10.1159/000492559

5. Perello M, Dickson SL (2015) Ghrelin signalling on food reward: a salient link between the gut and the mesolimbic system. J Neuroendocrinol 27:424–434. https://doi.org/10.1111/jne.12236

6. Yanagi S, Sato T, Kangawa K, Nakazato M (2018) The Homeostatic Force of Ghrelin. Cell Metab 27:786–804. https://doi.org/10.1016/j.cmet.2018.02.008

7. Wang Q, Liu C, Uchida A, et al (2014) Arcuate AgRP neurons mediate orexigenic and glucoregulatory actions of ghrelin. Mol Metab 3:64–72. https://doi.org/10.1016/j.molmet.2013.10.001

8. Atasoy D, Betley JN, Su HH, Sternson SM (2012) Deconstruction of a neural circuit for hunger. Nature 488:172–177. https://doi.org/10.1038/nature11270

9. Alcantara IC, Tapia APM, Aponte Y, Krashes MJ (2022) Acts of appetite: neural circuits governing the appetitive, consummatory, and terminating phases of feeding. Nat Metab 4:836–847. https://doi.org/10.1038/s42255-022-00611-y

10. Howard AD, Feighner SD, Cully DF, et al (1996) A receptor in pituitary and hypothalamus that functions in growth hormone release. Science 273:974–977. https://doi.org/10.1126/science.273.5277.974

11. Willesen MG, Kristensen P, Rømer J (1999) Co-localization of growth hormone secretagogue receptor and NPY mRNA in the arcuate nucleus of the rat. Neuroendocrinology 70:306–316. https://doi.org/10.1159/000054491

12. Abizaid A, Liu Z-W, Andrews ZB, et al (2006) Ghrelin modulates the activity and synaptic input organization of midbrain dopamine neurons while promoting appetite. J Clin Invest 116:3229–3239. https://doi.org/10.1172/JCI29867

13. Mp C, F B, D C, et al (2020) Growth hormone secretagogue receptor in dopamine neurons controls appetitive and consummatory behaviors towards high-fat diet in ad-libitum fed mice. Psychoneuroendocrinology 119:. https://doi.org/10.1016/j.psyneuen.2020.104718

14. Al Massadi O, Nogueiras R, Dieguez C, Girault J-A (2019) Ghrelin and food reward. Neuropharmacology 148:131–138. https://doi.org/10.1016/j.neuropharm.2019.01.001

15. Aguggia JP, Cornejo MP, Fernandez G, et al (2022) Growth hormone secretagogue receptor signaling in the supramammillary nucleus targets nitric oxide-producing neurons and controls recognition memory in mice. Psychoneuroendocrinology 139:105716. https://doi.org/10.1016/j.psyneuen.2022.105716

16. Cornejo MP, Barrile F, De Francesco PN, et al (2018) Ghrelin Recruits Specific Subsets of Dopamine and GABA Neurons of Different Ventral Tegmental Area Sub-nuclei. Neuroscience 392:107–120. https://doi.org/10.1016/j.neuroscience.2018.09.027

17. López-Ferreras L, Richard JE, Anderberg RH, et al (2017) Ghrelin's control of food reward and body weight in the lateral hypothalamic area is sexually dimorphic. Physiol Behav 176:40–49. https://doi.org/10.1016/j.physbeh.2017.02.011

18. Olszewski PK, Li D, Grace MK, et al (2003) Neural basis of orexigenic effects of ghrelin acting within lateral hypothalamus. Peptides 24:597–602. https://doi.org/10.1016/s0196-9781(03)00105-0

19. Anand BK, Brobeck JR (1951) Localization of a "feeding center" in the hypothalamus of the rat. Proc Soc Exp Biol Med 77:323–324. https://doi.org/10.3181/00379727-77-18766

20. Morrison SD, Barrnett RJ, Mayer J (1958) Localization of lesions in the lateral hypothalamus of rats with induced adipsia and aphagia. Am J Physiol 193:230–234. https://doi.org/10.1152/ajplegacy.1958.193.1.230

21. Saper CB, Swanson LW, Cowan WM (1979) An autoradiographic study of the efferent connections of the lateral hypothalamic area in the rat. J Comp Neurol 183:689–706. https://doi.org/10.1002/cne.901830402

22. Hahn JD, Swanson LW (2010) Distinct patterns of neuronal inputs and outputs of the juxtaparaventricular and suprafornical regions of the lateral hypothalamic area in the male rat. Brain Res Rev 64:14–103. https://doi.org/10.1016/j.brainresrev.2010.02.002

23. Wang Y, Eddison M, Fleishman G, et al (2021) EASI-FISH for thick tissue defines lateral hypothalamus spatio-molecular organization. Cell 184:6361-6377.e24. https://doi.org/10.1016/j.cell.2021.11.024

24. Guan XM, Yu H, Palyha OC, et al (1997) Distribution of mRNA encoding the growth hormone secretagogue receptor in brain and peripheral tissues. Brain Res Mol Brain Res 48:23–29. https://doi.org/10.1016/s0169-328x(97)00071-5

25. Mitchell V, Bouret S, Beauvillain JC, et al (2001) Comparative distribution of mRNA encoding the growth hormone secretagogue-receptor (GHS-R) in Microcebus murinus (Primate,

lemurian) and rat forebrain and pituitary. J Comp Neurol 429:469–489. https://doi.org/10.1002/1096-9861(20010115)429:3<469::aid-cne8>3.0.co;2-#

26. Zigman JM, Jones JE, Lee CE, et al (2006) Expression of ghrelin receptor mRNA in the rat and the mouse brain. J Comp Neurol 494:528–548. https://doi.org/10.1002/cne.20823

27. Mani BK, Osborne-Lawrence S, Mequinion M, et al (2017) The role of ghrelin-responsive mediobasal hypothalamic neurons in mediating feeding responses to fasting. Mol Metab 6:882–896. https://doi.org/10.1016/j.molmet.2017.06.011

28. Mani BK, Walker AK, Lopez Soto EJ, et al (2014) Neuroanatomical characterization of a growth hormone secretagogue receptor-green fluorescent protein reporter mouse. The Journal of comparative neurology 522:3644–3666. https://doi.org/10.1002/cne.23627

29. Wren AM, Small CJ, Abbott CR, et al (2001) Ghrelin causes hyperphagia and obesity in rats. Diabetes 50:2540–2547. https://doi.org/10.2337/diabetes.50.11.2540

30. Toshinai K, Date Y, Murakami N, et al (2003) Ghrelin-induced food intake is mediated via the orexin pathway. Endocrinology 144:1506–1512. https://doi.org/10.1210/en.2002-220788

31. Scott V, McDade DM, Luckman SM (2007) Rapid changes in the sensitivity of arcuate nucleus neurons to central ghrelin in relation to feeding status. Physiol Behav 90:180–185. https://doi.org/10.1016/j.physbeh.2006.09.026

32. Cabral A, Valdivia S, Fernandez G, et al (2014) Divergent neuronal circuitries underlying acute orexigenic effects of peripheral or central ghrelin: critical role of brain accessibility. J Neuroendocrinol 26:542–554. https://doi.org/10.1111/jne.12168

33. Lawrence CB, Snape AC, Baudoin FM-H, Luckman SM (2002) Acute central ghrelin and GH secretagogues induce feeding and activate brain appetite centers. Endocrinology 143:155–162. https://doi.org/10.1210/endo.143.1.8561

34. Perello M, Sakata I, Birnbaum S, et al (2010) Ghrelin increases the rewarding value of high-fat diet in an orexin-dependent manner. Biol Psychiatry 67:880–886. https://doi.org/10.1016/j.biopsych.2009.10.030

35. van den Pol AN, Yao Y, Fu L-Y, et al (2009) Neuromedin B and gastrin-releasing peptide excite arcuate nucleus neuropeptide Y neurons in a novel transgenic mouse expressing strong Renilla green fluorescent protein in NPY neurons. J Neurosci 29:4622–4639. https://doi.org/10.1523/JNEUROSCI.3249-08.2009

36. Madisen L, Zwingman TA, Sunkin SM, et al (2010) A robust and high-throughput Cre reporting and characterization system for the whole mouse brain. Nature Neuroscience 13:133–140. https://doi.org/10.1038/nn.2467

37. Taniguchi H, He M, Wu P, et al (2011) A resource of Cre driver lines for genetic targeting of GABAergic neurons in cerebral cortex. Neuron 71:995–1013. https://doi.org/10.1016/j.neuron.2011.07.026

38. Taniguchi H, He M, Wu P, et al (2011) A resource of Cre driver lines for genetic targeting of GABAergic neurons in cerebral cortex. Neuron 71:995–1013. https://doi.org/10.1016/j.neuron.2011.07.026

39. Cabral A, Suescun O, Zigman JM, Perello M (2012) Ghrelin indirectly activates hypophysiotropic CRF neurons in rodents. PloS one 7:e31462. https://doi.org/10.1371/journal.pone.0031462

40. Chuang J-C, Sakata I, Kohno D, et al (2011) Ghrelin directly stimulates glucagon secretion from pancreatic alpha-cells. Mol Endocrinol 25:1600–1611. https://doi.org/10.1210/me.2011-1001

41. Cardona A, Saalfeld S, Schindelin J, et al (2012) TrakEM2 software for neural circuit reconstruction. PLoS ONE 7:e38011. https://doi.org/10.1371/journal.pone.0038011

42. Ester M, Kriegel H, Sander J, Xu X (1996) A density-based algorithm for discovering clusters in large spatial databases with noise. AAAI Press, pp 226–231

43. Wang Q, Ding S-L, Li Y, et al (2020) The Allen Mouse Brain Common Coordinate Framework: A 3D Reference Atlas. Cell 181:936-953.e20. https://doi.org/10.1016/j.cell.2020.04.007

44. Cabral A, Portiansky E, Sánchez-Jaramillo E, et al (2016) Ghrelin activates hypophysiotropic corticotropin-releasing factor neurons independently of the arcuate nucleus. Psychoneuroendocrinology 67:27–39. https://doi.org/10.1016/j.psyneuen.2016.01.027

45. Cornejo MP, De Francesco PN, García Romero G, et al (2018) Ghrelin receptor signaling targets segregated clusters of neurons within the nucleus of the solitary tract. Brain Structure and Function 223:3133–3147. https://doi.org/10.1007/s00429-018-1682-5

46. Uriarte M, De Francesco PN, Fernández G, et al (2021) Circulating ghrelin crosses the blood-cerebrospinal fluid barrier via growth hormone secretagogue receptor dependent and independent mechanisms. Molecular and cellular endocrinology 538:111449. https://doi.org/10.1016/j.mce.2021.111449

47. Bernardis LL, Bellinger LL (1993) The lateral hypothalamic area revisited: neuroanatomy, body weight regulation, neuroendocrinology and metabolism. Neurosci Biobehav Rev 17:141–193. https://doi.org/10.1016/s0149-7634(05)80149-6

48. Paxinos and Franklin (2001) The Mouse Brain in Stereotaxic Coordinates

49. Abercrombie M (1946) Estimation of nuclear population from microtome sections. The Anatomical Record 94:239–247

50. Lein ES, Hawrylycz MJ, Ao N, et al (2007) Genome-wide atlas of gene expression in the adult mouse brain. Nature 445:168–176. https://doi.org/10.1038/nature05453

51. Godfrey N, Borgland SL (2019) Diversity in the lateral hypothalamic input to the ventral tegmental area. Neuropharmacology 154:4–12. https://doi.org/10.1016/j.neuropharm.2019.05.014

52. Aponte Y, Atasoy D, Sternson SM (2011) AGRP neurons are sufficient to orchestrate feeding behavior rapidly and without training. Nat Neurosci 14:351–355. https://doi.org/10.1038/nn.2739

53. Burt J, Alberto CO, Parsons MP, Hirasawa M (2011) Local network regulation of orexin neurons in the lateral hypothalamus. Am J Physiol Regul Integr Comp Physiol 301:R572-580. https://doi.org/10.1152/ajpregu.00674.2010

54. Cone JJ, McCutcheon JE, Roitman MF (2014) Ghrelin acts as an interface between physiological state and phasic dopamine signaling. J Neurosci 34:4905–4913. https://doi.org/10.1523/JNEUROSCI.4404-13.2014

55. Szentirmai E, Kapás L, Krueger JM (2007) Ghrelin microinjection into forebrain sites induces wakefulness and feeding in rats. Am J Physiol Regul Integr Comp Physiol 292:R575-585. https://doi.org/10.1152/ajpregu.00448.2006

56. Theander-Carrillo C, Wiedmer P, Cettour-Rose P, et al (2006) Ghrelin action in the brain controls adipocyte metabolism. J Clin Invest 116:1983–1993. https://doi.org/10.1172/JCI25811

57. Abtahi S, Mirza A, Howell E, Currie PJ (2017) Ghrelin enhances food intake and carbohydrate oxidation in a nitric oxide dependent manner. Gen Comp Endocrinol 250:9–14. https://doi.org/10.1016/j.ygcen.2017.05.017

58. Cui RJ, Li X, Appleyard SM (2011) Ghrelin inhibits visceral afferent activation of catecholamine neurons in the solitary tract nucleus. J Neurosci 31:3484–3492. https://doi.org/10.1523/JNEUROSCI.3187-10.2011

59. Feng DD, Yang S-K, Loudes C, et al (2011) Ghrelin and obestatin modulate growth hormone-releasing hormone release and synaptic inputs onto growth hormone-releasing hormone neurons. Eur J Neurosci 34:732–744. https://doi.org/10.1111/j.1460-9568.2011.07787.x

60. Suarez AN, Liu CM, Cortella AM, et al (2020) Ghrelin and Orexin Interact to Increase Meal Size Through a Descending Hippocampus to Hindbrain Signaling Pathway. Biol Psychiatry 87:1001–1011. https://doi.org/10.1016/j.biopsych.2019.10.012

61. Peyron C, Tighe DK, van den Pol AN, et al (1998) Neurons containing hypocretin (orexin) project to multiple neuronal systems. J Neurosci 18:9996–10015. https://doi.org/10.1523/JNEUROSCI.18-23-09996.1998

62. Bäckberg M, Hervieu G, Wilson S, Meister B (2002) Orexin receptor-1 (OX-R1) immunoreactivity in chemically identified neurons of the hypothalamus: focus on orexin targets involved in control of food and water intake. Eur J Neurosci 15:315–328. https://doi.org/10.1046/j.0953-816x.2001.01859.x

63. Kohno D, Gao H-Z, Muroya S, et al (2003) Ghrelin directly interacts with neuropeptide-Y-containing neurons in the rat arcuate nucleus: Ca2+ signaling via protein kinase A and N-type channel-dependent mechanisms and cross-talk with leptin and orexin. Diabetes 52:948–956. https://doi.org/10.2337/diabetes.52.4.948

64. Date Y, Ueta Y, Yamashita H, et al (1999) Orexins, orexigenic hypothalamic peptides, interact with autonomic, neuroendocrine and neuroregulatory systems. Proc Natl Acad Sci U S A 96:748–753. https://doi.org/10.1073/pnas.96.2.748

65. Mickelsen LE, Kolling FW, Chimileski BR, et al (2017) Neurochemical Heterogeneity Among Lateral Hypothalamic Hypocretin/Orexin and Melanin-Concentrating Hormone Neurons Identified Through Single-Cell Gene Expression Analysis. eNeuro 4:ENEURO.0013-17.2017. https://doi.org/10.1523/ENEURO.0013-17.2017

66. Yamanaka A, Beuckmann CT, Willie JT, et al (2003) Hypothalamic orexin neurons regulate arousal according to energy balance in mice. Neuron 38:701–713. https://doi.org/10.1016/s0896-6273(03)00331-3

67. Brown JA, Bugescu R, Mayer TA, et al (2017) Loss of Action via Neurotensin-Leptin Receptor Neurons Disrupts Leptin and Ghrelin-Mediated Control of Energy Balance. Endocrinology 158:1271–1288. https://doi.org/10.1210/en.2017-00122

68. Li S-B, de Lecea L (2020) The hypocretin (orexin) system: from a neural circuitry perspective. Neuropharmacology 167:107993. https://doi.org/10.1016/j.neuropharm.2020.107993

69. Feldblum S, Erlander MG, Tobin AJ (1993) Different distributions of GAD65 and GAD67 mRNAs suggest that the two glutamate decarboxylases play distinctive functional roles. J Neurosci Res 34:689–706. https://doi.org/10.1002/jnr.490340612

70. Yamakawa T, Kurauchi Y, Hisatsune A, et al (2018) Endogenous Nitric Oxide Inhibits, Whereas Awakening Stimuli Increase, the Activity of a Subset of Orexin Neurons. Biol Pharm Bull 41:1859–1865. https://doi.org/10.1248/bpb.b18-00633

71. Cador M, Kelley AE, Le Moal M, Stinus L (1986) Ventral tegmental area infusion of substance P, neurotensin and enkephalin: differential effects on feeding behavior. Neuroscience 18:659–669. https://doi.org/10.1016/0306-4522(86)90061-8

72. Jordan LM (1998) Initiation of locomotion in mammals. Ann N Y Acad Sci 860:83–93. https://doi.org/10.1111/j.1749-6632.1998.tb09040.x

73. Sinnamon HM (1993) Preoptic and hypothalamic neurons and the initiation of locomotion in the anesthetized rat. Prog Neurobiol 41:323–344. https://doi.org/10.1016/0301-0082(93)90003-b

74. van den Pol AN (1999) Hypothalamic hypocretin (orexin): robust innervation of the spinal cord. J Neurosci 19:3171–3182. https://doi.org/10.1523/JNEUROSCI.19-08-03171.1999

75. Bonnavion P, Mickelsen LE, Fujita A, et al (2016) Hubs and spokes of the lateral hypothalamus: cell types, circuits and behaviour. J Physiol 594:6443–6462. https://doi.org/10.1113/JP271946

76. Karnani MM, Schöne C, Bracey EF, et al (2020) Role of spontaneous and sensory orexin network dynamics in rapid locomotion initiation. Prog Neurobiol 187:101771. https://doi.org/10.1016/j.pneurobio.2020.101771

77. Concetti C, Burdakov D (2021) Orexin/Hypocretin and MCH Neurons: Cognitive and Motor Roles Beyond Arousal. Front Neurosci 15:639313. https://doi.org/10.3389/fnins.2021.639313

78. De Francesco PN, Fernandez G, Uriarte M, et al (2023) Systemic Ghrelin Treatment Induces Rapid, Transient, and Asymmetric Changes in the Metabolic Activity of the Mouse Brain. Neuroendocrinology 113:64–79. https://doi.org/10.1159/000526245

79. Cabral A, Cornejo MP, Fernandez G, et al (2017) Circulating Ghrelin Acts on GABA Neurons of the Area Postrema and Mediates Gastric Emptying in Male Mice. Endocrinology 158:1436–1449. https://doi.org/10.1210/en.2016-1815

80. Perello M, Cabral A, Cornejo MP, et al (2019) Brain accessibility delineates the central effects of circulating ghrelin. J Neuroendocrinol 31:e12677. https://doi.org/10.1111/jne.12677

81. Schaeffer M, Langlet F, Lafont C, et al (2013) Rapid sensing of circulating ghrelin by hypothalamic appetite-modifying neurons. Proc Natl Acad Sci U S A 110:1512–1517. https://doi.org/10.1073/pnas.1212137110

82. Uriarte M, De Francesco PN, Fernandez G, et al (2019) Evidence Supporting a Role for the Blood-Cerebrospinal Fluid Barrier Transporting Circulating Ghrelin into the Brain. Mol Neurobiol 56:4120–4134. https://doi.org/10.1007/s12035-018-1362-8

83. Cabral A, López Soto EJ, Epelbaum J, Perelló M (2017) Is Ghrelin Synthesized in the Central Nervous System? Int J Mol Sci 18:638. https://doi.org/10.3390/ijms18030638

84. Cornejo MP, Mustafá ER, Cassano D, et al (2021) The ups and downs of growth hormone secretagogue receptor signaling. FEBS J 288:7213–7229. https://doi.org/10.1111/febs.15718

85. M'Kadmi C, Cabral A, Barrile F, et al (2019) N-Terminal Liver-Expressed Antimicrobial Peptide 2 (LEAP2) Region Exhibits Inverse Agonist Activity toward the Ghrelin Receptor. J Med Chem 62:965–973. https://doi.org/10.1021/acs.jmedchem.8b01644

86. Clegg DJ, Brown LM, Zigman JM, et al (2007) Estradiol-dependent decrease in the orexigenic potency of ghrelin in female rats. Diabetes 56:1051–1058. https://doi.org/10.2337/db06-0015

87. de Souza GO, Wasinski F, Donato J (2022) Characterization of the metabolic differences between male and female C57BL/6 mice. Life Sci 301:120636. https://doi.org/10.1016/j.lfs.2022.120636

88. Ben-Barak Y, Russell JT, Whitnall MH, et al (1985) Neurophysin in the hypothalamo-neurohypophysial system. I. Production and characterization of monoclonal antibodies. J Neurosci 5:81–97. https://doi.org/10.1523/JNEUROSCI.05-01-00081.1985

89. Perello M, Stuart RC, Vaslet CA, Nillni EA (2007) Cold exposure increases the biosynthesis and proteolytic processing of prothyrotropin-releasing hormone in the hypothalamic paraventricular nucleus via beta-adrenoreceptors. Endocrinology 148:4952–4964. https://doi.org/10.1210/en.2007-0522

Figure 1

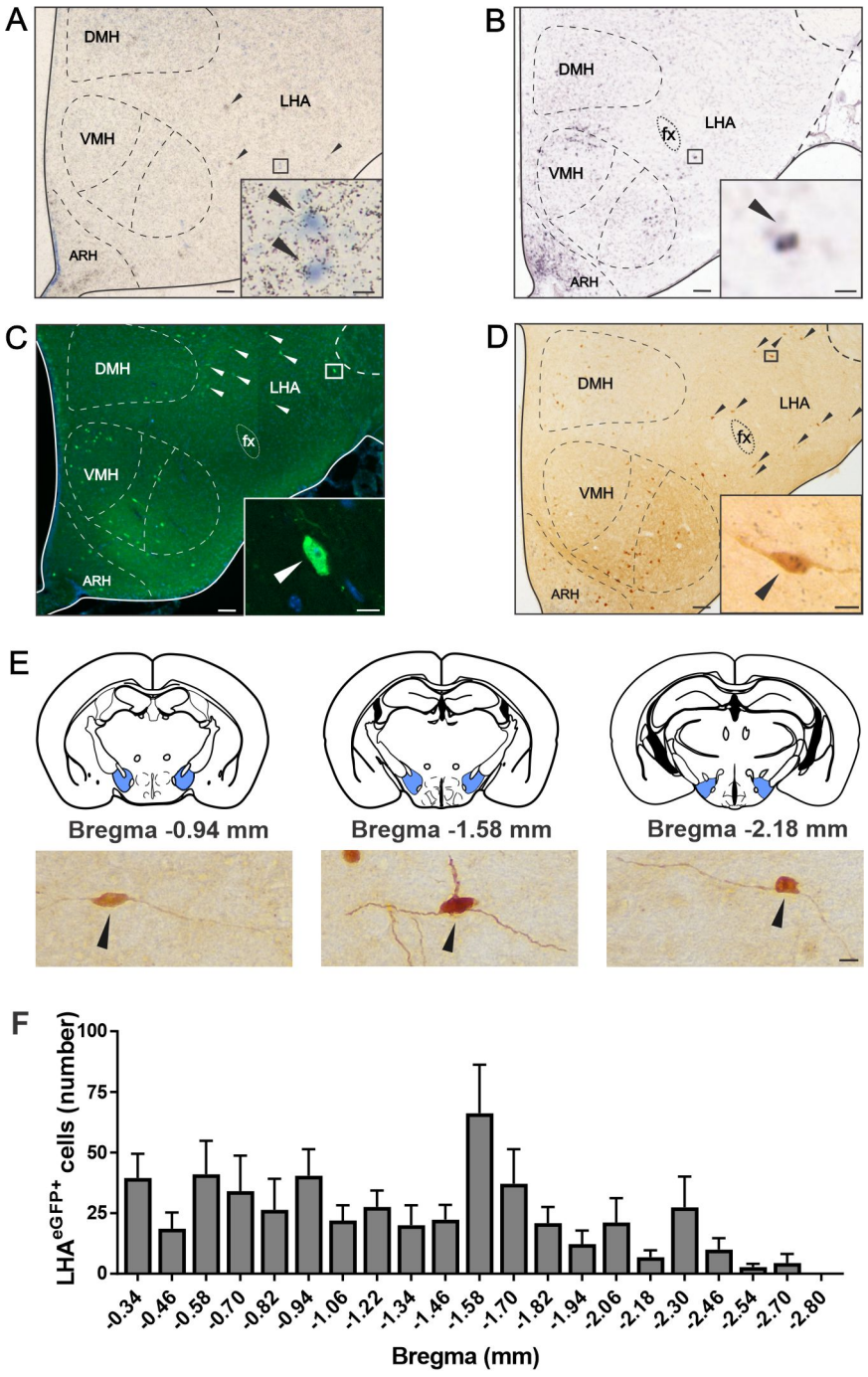
A
DMH
LHA
VMH
ARH
B
DMH
LHA
fx
VMH
ARH
C
DMH
LHA
fx
VMH
ARH
D
DMH
LHA
fx
VMH
ARH
E
Bregma -0.94 mm
Bregma -1.58 mm
Bregma -2.18 mm
F
LHA^eGFP+ cells (number)
100
75
50
25
0
-0.34
-0.46
-0.58
-0.70
-0.82
-0.94
-1.06
-1.22
-1.34
-1.46
-1.58
-1.70
-1.82
-1.94
-2.06
-2.18
-2.30
-2.46
-2.54
-2.70
-2.80
Bregma (mm)

Figure 2

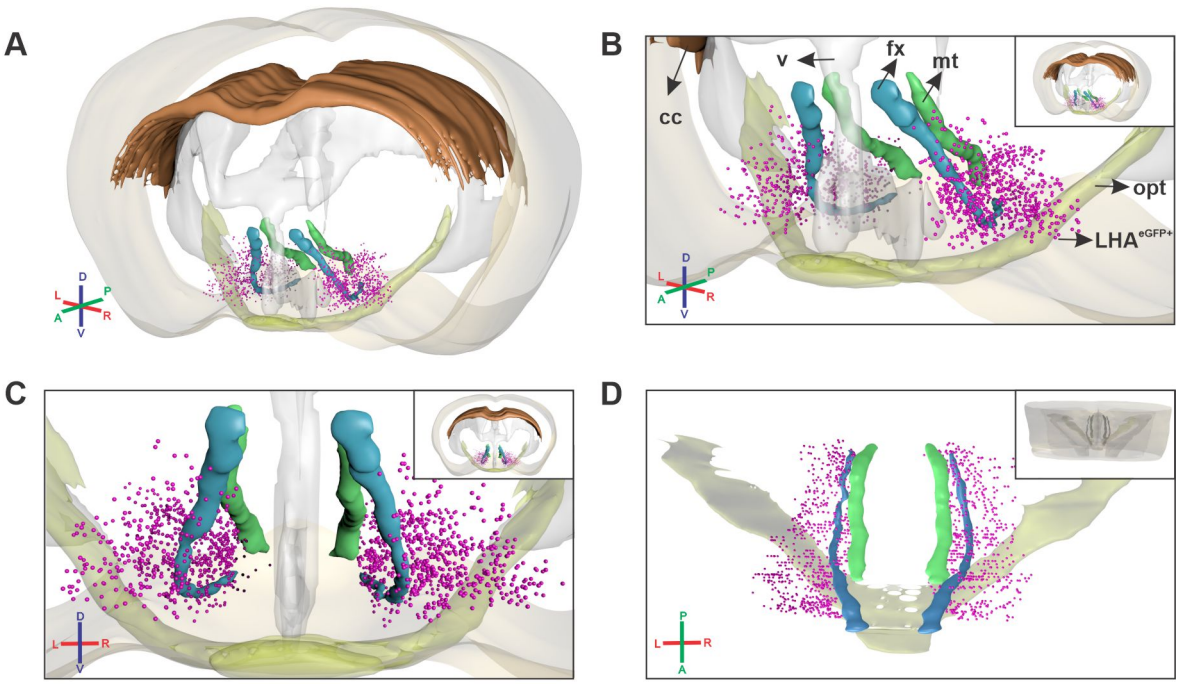

Figure 3

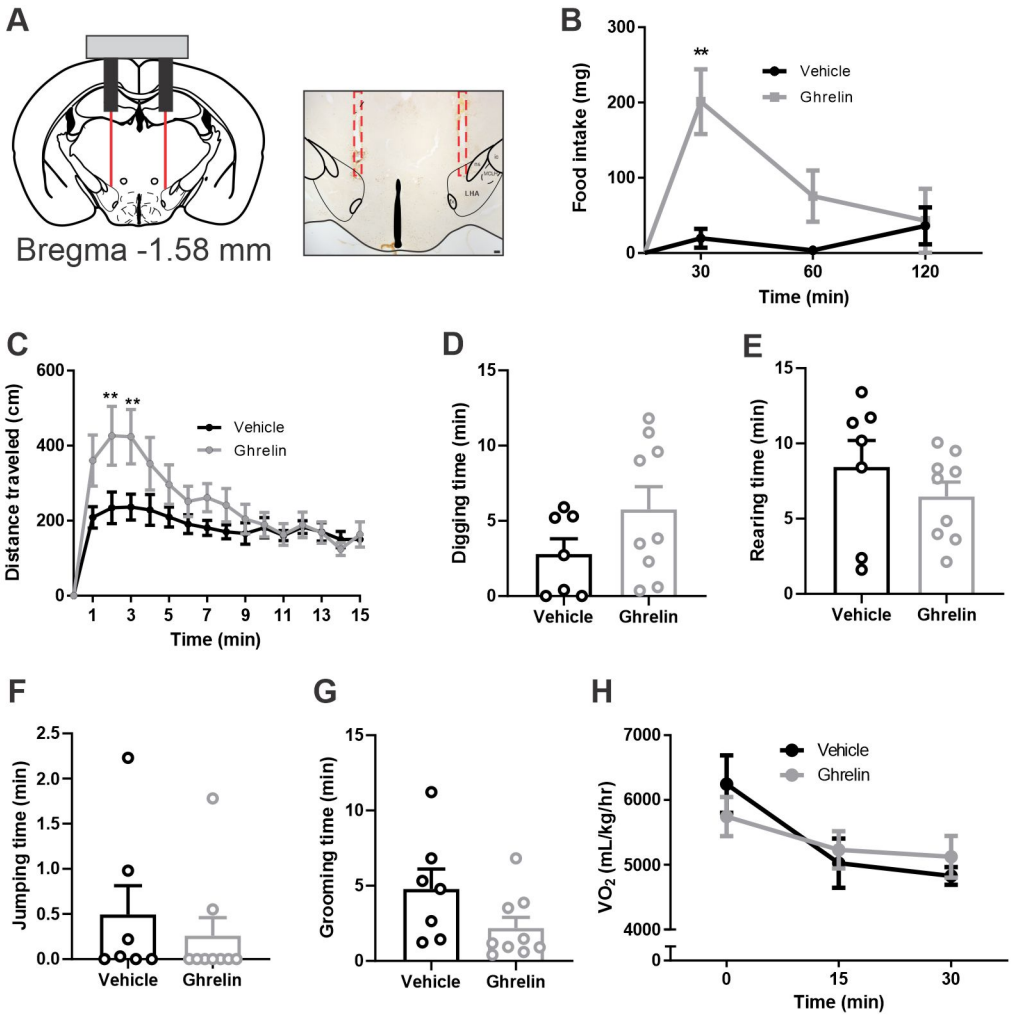
A
Bregma -1.58 mm
LHA
B
Food intake (mg)
300
200
100
0
**
Vehicle
Ghrelin
30
60
120
Time (min)
C
Distance traveled (cm)
600
400
200
0
** **
Vehicle
Ghrelin
1
3
5
7
9
11
13
15
Time (min)
D
Digging time (min)
15
10
5
0
Vehicle
Ghrelin
E
Rearing time (min)
15
10
5
0
Vehicle
Ghrelin
F
Jumping time (min)
2.5
2.0
1.5
1.0
0.5
0.0
Vehicle
Ghrelin
G
Grooming time (min)
15
10
5
0
Vehicle
Ghrelin
H
VO2 (mL/kg/hr)
7000
6000
5000
4000
0
Vehicle
Ghrelin
0
15
30
Time (min)

Figure 4

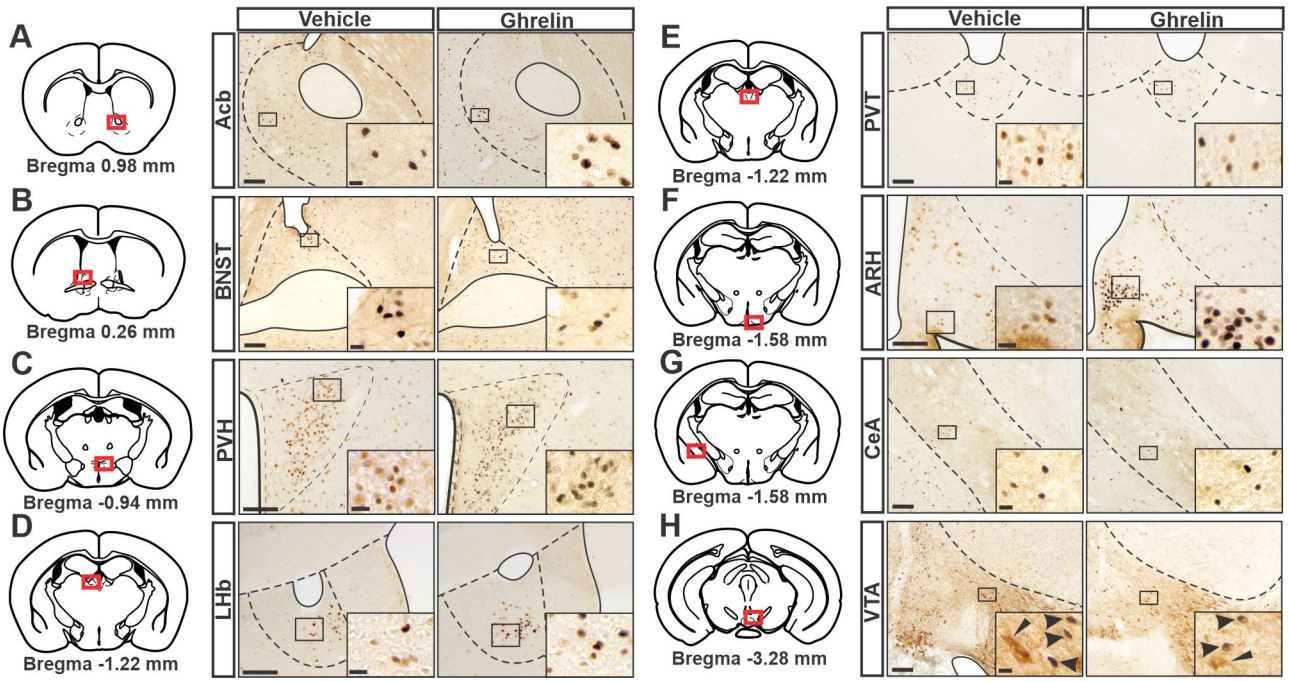
A
Bregma 0.98 mm
B
Bregma 0.26 mm
C
Bregma -0.94 mm
D
Bregma -1.22 mm
Vehicle
Ghrelin
Acb
BNST
PVH
LHb
E
Bregma -1.22 mm
F
Bregma -1.58 mm
G
Bregma -1.58 mm
H
Bregma -3.28 mm
Vehicle
Ghrelin
PVT
ARH
CeA
VTA

Figure 5

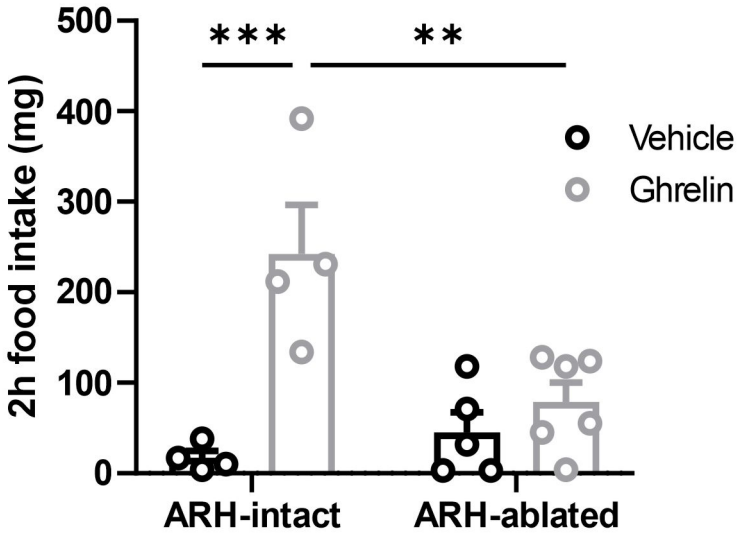
500
400
300
200
100
0
2h food intake (mg)
***
**
Vehicle
Ghrelin
ARH-intact
ARH-ablated

Figure 6

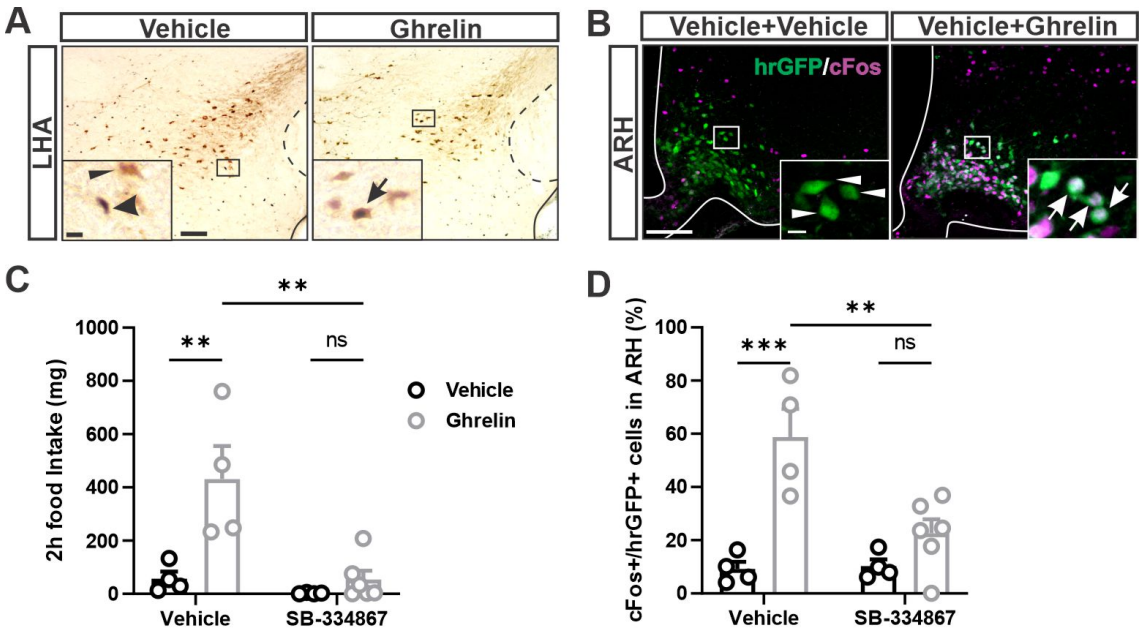
A
Vehicle
Ghrelin
LHA
B
Vehicle+Vehicle
Vehicle+Ghrelin
ARH
hrGFP/cFos
C
2h food Intake (mg)
1000
800
600
400
200
0
**
**
ns
Vehicle
Ghrelin
Vehicle
SB-334867
D
cFos+/hrGFP+ cells in ARH (%)
100
80
60
40
20
0
**
***
ns
Vehicle
SB-334867

Figure 7

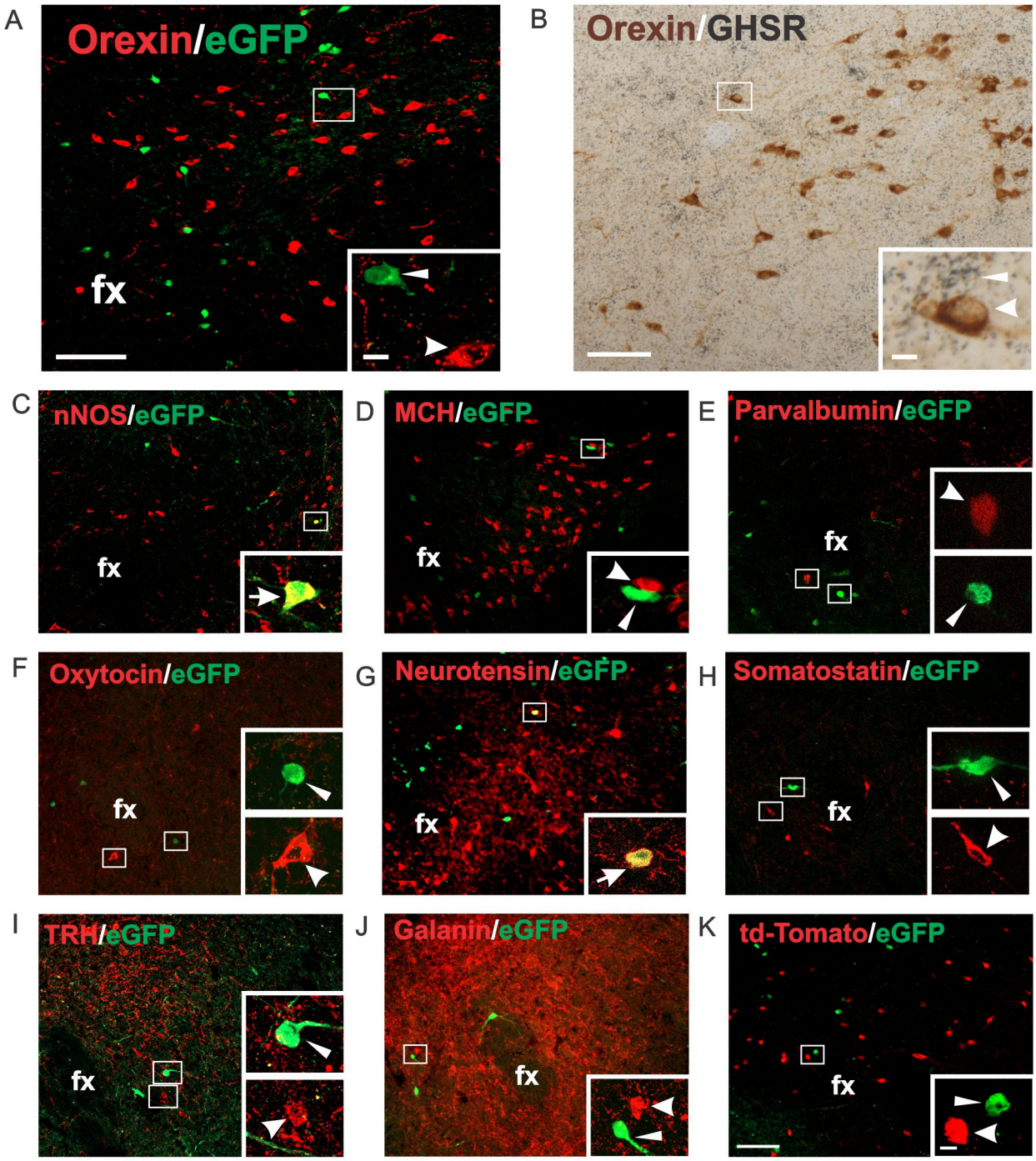
A
Orexin/eGFP
fx
B
Orexin/GHSR
C
nNOS/eGFP
fx
D
MCH/eGFP
fx
E
Parvalbumin/eGFP
fx
F
Oxytocin/eGFP
fx
G
Neurotensin/eGFP
fx
H
Somatostatin/eGFP
fx
I
TRH/eGFP
fx
J
Galanin/eGFP
fx
K
td-Tomato/eGFP
fx

Figure 8

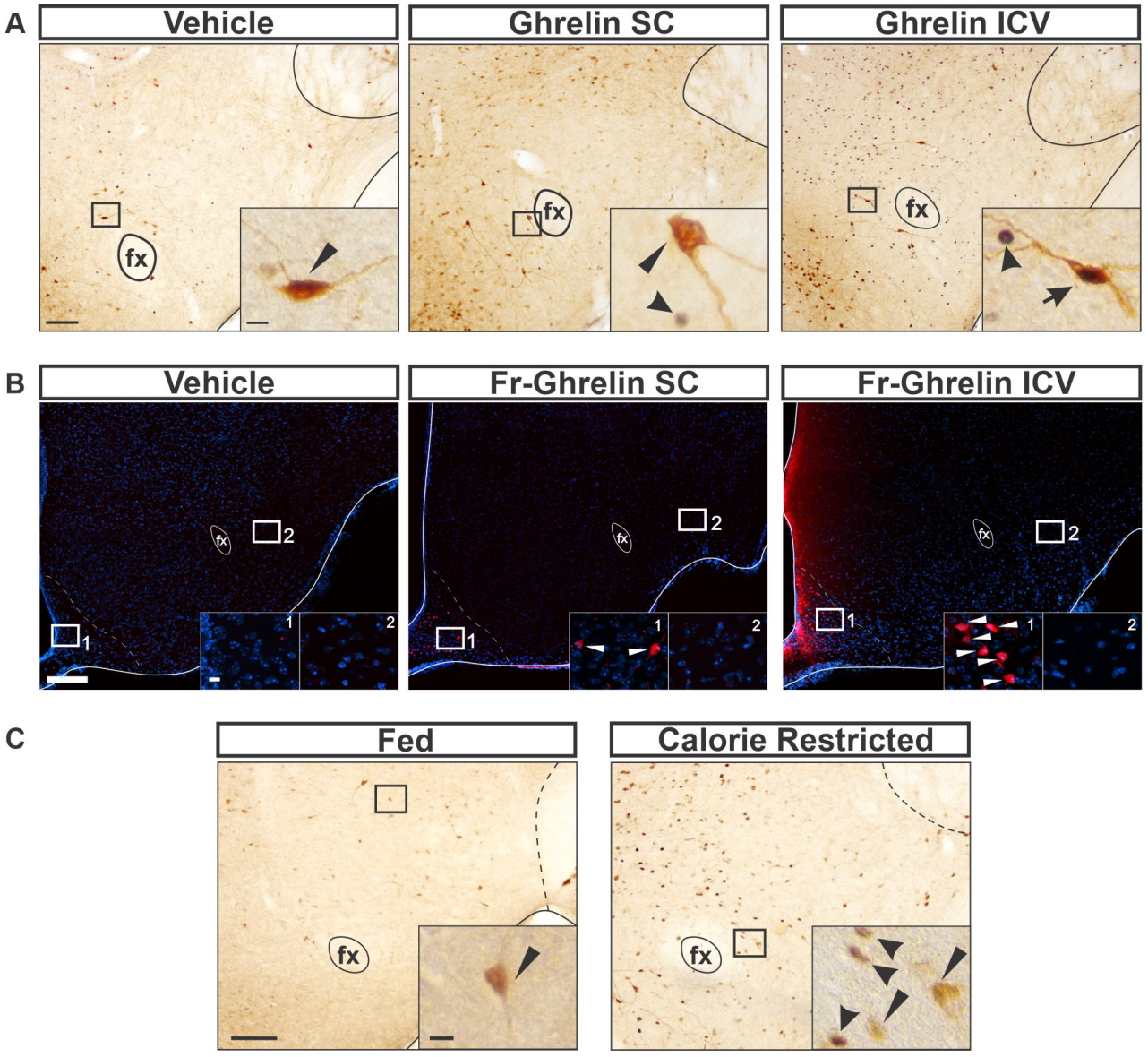
A
Vehicle
Ghrelin SC
Ghrelin ICV
fx
B
Vehicle
Fr-Ghrelin SC
Fr-Ghrelin ICV
fx
1
2
C
Fed
Calorie Restricted
fx

Figure 9

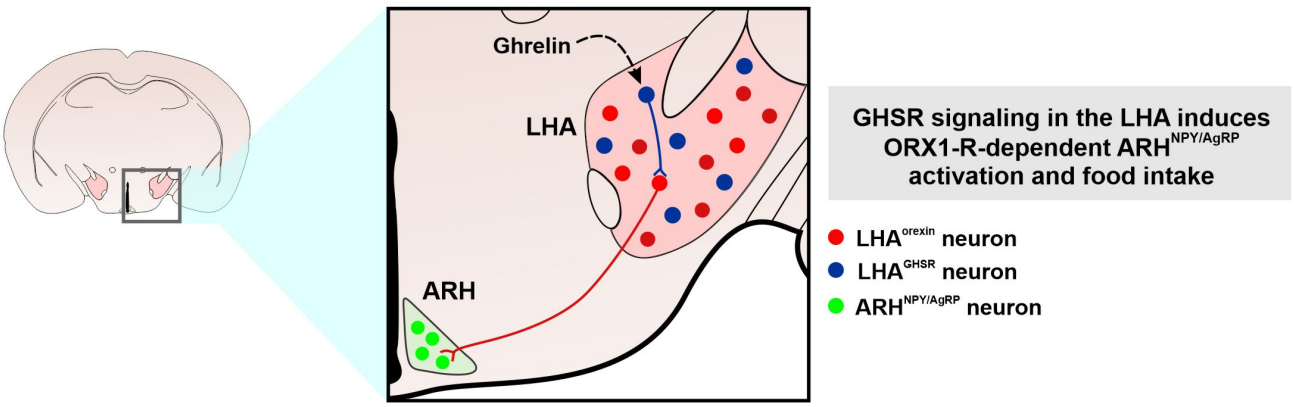
Ghrelin
LHA
ARH
GHSR signaling in the LHA induces ORX1-R-dependent ARH NPY/AgRP activation and food intake
LHA orexin neuron
LHA GHSR neuron
ARH NPY/AgRP neuron

Supplementary figure 1